Lehigh University
Lehigh Preserve

Theses and Dissertations

1-1-1983

Maximum strength of ship hulls subjected to moment, torque and shear.

Thomas R. Moore

Follow this and additional works at: http://preserve.lehigh.edu/etd

Part of the Civil Engineering Commons

Recommended Citation

Moore, Thomas R., "Maximum strength of ship hulls subjected to moment, torque and shear." (1983). *Theses and Dissertations.* Paper 2463.

MAXIMUM STRENGTH OF SHIP HULLS

SUBJECTED TO

MOMENT, TORQUE AND SHEAR

by

Thomas R. Moore

A Thesis

Presented to the Graduate Committee

of Lehigh University

in Candidacy for the Degree of

Master of Science
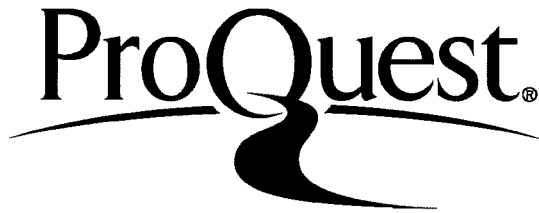

in

Civil Engineering

Lehigh University

1983

ProQuest Number: EP76740

ProQuest EP76740

This thesis is accepted and approved in partial fulfillment of the requirements for the degree of Master of Science.

January 26, 1983
(date)

_____
Professor in Charge

_____
Chairman of Department

ii

ACKNOWLEDGMENTS

ACKNOWLEDGMENTS

Table of Contents

v

LIST OF TABLES

LIST OF FIGURES

ABSTRACT

This report describes a method for determining the ultimate strength and behavior of longitudinally stiffened ship hull girders of single-cell cross section subjected to moment, torque and shear.

The compression flange is assumed to behave as if it were composed of parallel beam-columns whose axial load deformation relationship is established by another computer program. Axial response of the other components in the section up to yielding or buckling is assumed to be of a bi-linear, elastic-plastic pattern. Multiple tension field action is assumed for the postbuckling shear response of the girder web subpanels. This method can maintain plane section or accommodate any degree of warping as specified by the user.

An efficient procedure was developed for this method to accelerate the iterative process of establishing equilibrium of forces on the cross section. This procedure has many potential applications other than in this method.

A comparison of this method with the results of twelve tests on box girder specimens (ship hull and bridge models) showed this method to be acceptably accurate for the combined loading of moment, torque and shear.

1

1. INTRODUCTION

1.1 Background and Related Research

A need for developing a reliable method of evaluating the maximum strength of ship hulls is becoming more important with the growing knowledge of ship loads. Although the traditional methods of ship analysis, which have evolved through years of practical experience, give adequately safe designs for common ship structures, it has been shown by full-scale tests and more exact analyses that the mechanisms of failure are often very different from the mechanisms predicted by these methods [30]. The major contributing factor to this discrepancy has been the nonlinear behavior of the individual components and subsequently of the entire hull system. The rapid introduction of novel ship types also requires a more rational approach to ship design than the semi-empirical traditional methods.

A considerable amount of research has been conducted on the ultimate strength and behavior of individual ship hull components such as individual plates [9, 11, 15], stiffened plates and grillages [10, 6, 1, 26, 24, 13, 7, 12, 20], and plate girders under shear and bending [16, 14, 31, 25]. Although knowledge of the behavior of these components is required for the analysis of a whole ship hull girder, only a limited amount of research has been devoted to the entire ship hull.

2

Caldwell proposed a direct solution for obtaining the ultimate bending strength of a hull girder section. This solution consisted of merely summing the ultimate strengths of the individual components [3]. The ultimate strength of the plate components was incorporated into the solution by means of the effective width, but the possibility of the post-ultimate reduction of the capacity was not considered. Thus, a summation of the individual ultimate strengths, as Caldwell proposed, may lead to a higher estimated capacity than the true strength.

Smith developed a method for obtaining the ultimate bending strength and behavior of a hull section [28]. Large deformations were considered for the components and the strain compatibility of the hull was enforced by maintaining a plane section. Although this method provided an adequate estimate of the bending capacity of a hull section, it could not accommodate the effects of shear or torque [4].

Herzog proposed a method for computing the bending strength of box girders by using greatly simplified strengths of the components [8].

Billingsley formulated a method which is similar to Smith's; however, it does not consider the post-ultimate behavior of individual components [2]. Again, this approach does not accommodate the effects of shear and torque.

3

A method was developed at Lehigh University for describing the behavior and predicting the ultimate strength of hull sections subjected to moment, shear, and torque [17, 19]. By considering large deflections of the compression flange, maintaining a plane section, and treating the side plating as the webs of a plate girder subjected to shear and moment, adequate results were obtained for cases involving shear and moment. However, for the cases involving torque the predictions of the ultimate strength were optimistic. This method was modified to allow curvature not only in the vertical plane but also in the horizontal plane, and to introduce the warping of the section as was measured in test specimens [21]. Although this modification improved the results for specimens with torque, the estimate was still too optimistic.

1.2 Purpose and Scope

The main purpose of the research presented here was to further develop the previous analytical method for determining the ultimate strength of longitudinally stiffened box girders of the scantlings typical for ship hulls and subjected to the combined action of moment, shear, and torque as shown in Fig. 1.

In the process of this work, the research results and computer programs which became available since the previous version of the method have been utilized [29, 19, 22].

The basic procedures of the original Lehigh method for

4

determining the behavior of the individual components were retained with some modifications. Components in tension are checked for yielding under the combination of shearing and normal stresses and the tension-field strength of web subpanels is computed by using a more recent approach than before. Also, more accurate computer programs are used for defining the axial behavior of the compression flange.

A very significant modification was made to the procedure for establishing the overall equilibrium of the cross section in terms of the corner strains and a prescribed degree of warping. In the previous version, a lengthy process involving incrementation and double parabolic interpolation was used. The new procedure leads to equilibrium in a few iterations. A study of the effect of warping showed that warping becomes significant after buckling of some of the web subpanels when the original symmetrical cross section is transformed into a structurally unsymmetrical one.

A comparison of theoretical and experimental results for twelve tests on box girder specimens indicated the method to be acceptably accurate.

2. THEORETICAL ANALYSIS

2.1 Assumptions

The proposed method of analysis incorporates the following simplifying assumptions:

1. Girder is straight and prismatic.

2. Cross section has a single-cell rectangular shape.

3. Strain distribution between corners of the section is linear.

4. The section maintains a constant degree of deplanation.

5. Material has a bilinear elastic-plastic stress-strain relationship. However, nonlinear materials can also be used by defining the stress-strain relationship with a series of points.

6. Transverse stiffeners are sufficiently rigid to provide unyielding support to the plating of the flanges and webs.

7. Effects of shear lag and distortion of the shape of the cross section are negligible.

Some additional specialized assumptions are stated as needed in the discussion of individual components.

The four component types used in the method are: compression flange elements (stiffener-plate combination), tension flange plate, longitudinal stiffeners of the tension flange and webs, and subpanels of the web plate. These components and the labeling system for the corners and webs are shown in Fig. 2.

6

2.2 Basic Stresses in the Box Girder Section

2.2.1 Effects of Moment and Shear

Prior to nonlinear behavior of individual girder elements, and if the effect of shear lag is neglected, the stresses in the box girder section due to moment and shear can be computed by using ordinary beam theory. The normal stresses vary linearly across the width of the flanges and the depth of the webs. The shearing stresses vary linearly in the flanges and are almost constant in the webs.

After some individual girder elements start behaving nonlinearly, the stress distribution changes as is shown in Fig. 3 and the analysis is performed under the following assumptions:

1. The non-linear axial response of the compression flange is adequately described by a series of points provided in advance (by another computer program or from a test).

2. The effect of shear on the compression flange is negligible.

3. The effect of shear on the tension flange is the reduction of the axial force required to yield the material.

4. After buckling, a web subpanel cannot carry any additional normal or bending stresses other than those present at buckling.

7

5. Shearing stresses are uniform in a particular subpanel and the postbuckling shear strength is developed by tension-field action.

2.2.2 Effect of torque

Since most of the torque in a girder with a closed cross section is carried by pure (St. Venant) torsion, even in the cases of cross sections restrained from warping [21], it is practical to neglect the shearing stresses due to warping. Then, the shear forces in the webs and flanges due to torque are:

Web: $\qquad V_{wt} = q_t \, d$ $\hspace{4cm}$ (2.1)

Flange: $\quad V_{ft} = q_t \, b$ $\hspace{4cm}$ (2.2)

where the shear flow q_t is given by

$$q_t = \frac{T}{2A_o} \hspace{4cm} (2.3)$$

with A_o being the enclosed area

$$A_o = b\ d \tag{2.4}$$

In reality, this situation changes after one of the components, usually a web subpanel, is significantly weakened. Then, the closed section is gradually transformed into an open section, with the "weak" component not fully participating in carrying additional torque. The shear center shifts and the additional torque must be primarily carried by warping stresses. The present version of the method does not consider the shifting of the shear center; however, it can accommodate the warping of the section.

2.3 Behavior of the Tension Flange Plate

The shear response of the tension flange plate is assumed to be linearly elastic with an unlimited shear strength. On the other hand, the axial response is assumed to be linearly elastic only until yielding under the combination of tension and shear according to the von Mises yield criterion.

$$S_{t\ max} = \sqrt{\frac{F_y^2}{3} - \tau^2} \tag{2.5}$$

9

This condition is checked in each subpanel of the tension flange plate.

2.4 Behavior of the Compression Flange

The compression flange of a hull girder segment is assumed to be adequately supported at the transverse stiffeners, and thus, consists of a longitudinally stiffened plate subjected to axial compression and possibly, lateral loading. The nonlinearity of the axial behavior of this plating arises from initial imperfections, welding residual stresses, buckling of the plate components, and lateral loading when it is present. The resultant overall strain and stress distributions across the width of the compression flange are shown in Fig. 3. The analysis is simplified by treating each stiffener with a portion of the plate as a separate element, in effect, a column under axial load. The method requires that the axial load response of such an element of the compression flange be defined for the pre- and post-ultimate ranges. Then the contribution of the whole compression flange is given by the sum of the contributions of the elements.

An individual compression flange element, consisting of a longitudinal stiffener and a portion of the plate with the width equal to the spacing of adjacent stiffeners is subjected to an axial load and the influence of the nonlinear effects mentioned

10

above. Its behavior is then identical to that of a beam-column like the one shown in Fig. 4.

Three separate computer programs were used to determine the axial behavior of the compression flange beam-columns. One was developed for the analysis of stiffened plate panels subjected to axial and lateral loads and having residual stresses in the plate [27]. The method was later modified to obtain the axial behavior with zero lateral loads, but it still did not consider initial imperfections and tended to be too optimistic [21]. The other program, based on the finite-element approach, includes consideration of residual stresses as well as of initial imperfections [28]. This method was found to be quite accurate in comparison with test results, but time consuming and not very reliable in the post-ultimate range. The third program is based on a rather simple design algorithm originally developed by multi-variable regression analysis of experimental and theoretical data [20]. In accuracy, this method was found to be close to the second method, yet it is much simpler and has no difficulties for the post-ultimate range. Figure 5 shows the stress-strain relationships produced by these three programs for the compression flange element of one of the test specimens [17].

2.5 Behavior of the Webs (Side Plating)

Up to the point of buckling of one of the plate subpanels, the web is assumed to behave linearly for shearing, bending, and normal stresses. Once buckling occurs in a subpanel, the postbuckling strength of this subpanel is assumed to develop independently from the other subpanels.

The ultimate shear capacity of the whole web is given by the sum of the ultimate shear strengths of the subpanels.

$$V_{wu} = \sum_{i=1}^{n} (V_{bi} + V_{tfi}) \qquad (2.6)$$

where

$$V_{bi} = \tau_{cri} d_i t_w = \text{buckling strength of the i-th subpanel} \qquad (2.7)$$

$$V_{tfi} = \tau_{tfi} d_i t_w = \text{tension field strength of the i-th subpanel} \qquad (2.8)$$

The critical shearing stress τ_{cri} [in Eq. (2.7)] of each subpanel is computed from the buckling interaction equation of the bending, normal, and shearing stresses.

12

$$\left[\frac{\tau_{cri}}{F_{vcri}}\right]^2 + \left[\frac{S_{bcri}}{F_{bcri}}\right]^2 + \frac{S_{ccri}}{F_{ccri}} \leqq 1.0 \qquad (2.9)$$

The pure buckling stresses F_{vcri}, F_{bcri}, and F_{ccri} given by the formulas of Table 1. There, the plate subpanels are assumed to be are simply supported on all four edges.

The shearing stress τ_{tfi} in Eq. (2.8) results from the formation of the tension field after buckling and is given by

$$\tau_{ti} = \frac{S_{ti}}{2\sqrt{1.0 + A_{min}(0.5 + A_{min})}} \qquad (2.10)$$

where

$$S_{ti} = F_y - \sqrt{0.25(S_{ccri} - S_{bcri})^2 + 3\tau_{cri}^2} \qquad (2.11)$$

is the tension field stress at the ultimate condition for the i-th subpanel and

$$A_{min} = \frac{a}{d_{i\ max}} \qquad (2.12)$$

13

is the aspect ratio of the widest subpanel. Thus, A_{min} is the same for all the subpanels [18].

Since the individual subpanels of the web usually have different widths d_i and are subjected to different combinations of bending and normal stresses, their buckling and the attainment of the ultimate condition occur at different stages of overall deformation of the web as shown in Fig.6 for a sample web with three subpanels.

Before buckling, deformation of each subpanel up to the point of buckling is linear and is readily defined by

$$r_{cri} = \frac{\tau'_{cri}}{G} \qquad\qquad (2.13)$$

where r is the shearing strain.

Since the postbuckling deformation cannot be accurately established, it is approximated with a straight line connecting the buckling deformation with the ultimate strength deformation. The ultimate deformation r_{ui} of the i-th subpanel is assumed to be reached when a diagonal fiber in the subpanel yields due to the racking distortion of the subpanel edges which are assumed to retain their original lengths. Thus,

14

$$r_{ui} = \frac{F_y}{E} \left[A_i + \frac{1}{A_i} \right] \qquad (2.14)$$

where

$$A_i = \frac{a}{d_i} \qquad (2.15)$$

Application of the above formulations at each of the kink points of the τ vs. r diagrams results in a continuous relationship between r and V for the whole web. In the process of computing this relationship it is important to keep in mind that, whereas the shear on a subpanel can increase, the normal and bending stresses are assumed to remain constant after buckling and, thus, the additional moment corresponding to the increase in the total web shear must be redistributed to the flanges, the web stiffeners and to the yet unbuckled web subpanels.

In the present version of the method, it is assumed that the longitudinal stiffeners in the webs are linearly elastic up to yielding. This assumption can be modified once the forces in the stiffeners due to the bending moment and the tension field action

are defined and the nonlinear behavior established.

2.6 Behavior and Ultimate Strength of the Girder

Once the load-deformation behavior of the individual components is defined, the analysis of the entire hull girder segment proceeds by enforcing compatibility between these components as the curvature of the girder is incremented. In summary, the following load-deformation relationships of the components are involved:

1. The nonlinear behavior of the individual beam-columns composing the compression flange. Each beam-column consists of a longitudinal stiffener and a portion of the compression flange plate. The load-deformation relationship for these beam-columns was obtained by using other computer programs.

2. The stiffeners of the tension flange and the web are assumed to be perfectly elastic-plastic.

3. The tension flange is assumed to be linearly elastic up to the point of yielding under the tensile and shearing stresses.

4. The webs of the girder are assumed to respond elastically up to the buckling or yielding of the plate subpanels. A buckled subpanel can carry more shear only by means of the tension field action. The bending and normal stresses, however, are assumed to remain at the buckling level.

16

In the course of establishing the load-deformation response of the girder segment, the method leads to many instances of iteration and thus becomes too time-consuming for manual computations. A computer program was written to overcome this difficulty. The present computer program is only for sections which are symmetrical about the vertical centroidal axis. However, this restriction is not a limitation of the method. The computer program is described in detail elsewhere [23]. Here is given only the general procedure of the method employed. The flowchart of Fig.7 shows the logic of the computer program BOX. The names in capital letters refer to the names of subroutines, such as, WVSDEF, PROPRT, etc., or to variables F, MY, and MX. The computational procedure can be explained by the following steps:

1. For a given value of curvature, the strains at the four corners of the cross section (Figs. 2 and 3) are calculated using an iterative process which makes the resultant axial force (F) and the bending moment about the vertical centroidal axis (MY) to become equal to zero. The strains are assumed to vary linearly on each side from corner to corner and the cross section is enforced to remain plane or to have the prescribed degree of warping.

2. After the equilibrium of the cross section is achieved for the given value of curvature, the bending moment about the

17

horizontal axis (MX) is calculated. Since the bending moment, shear, and torque are each related to a load parameter (W) by a constant, the values of the transverse shear (V) and the torque (T) can be readily computed.

$$W = MX/AMU2 \qquad (2.16)$$

$$\text{then,} \quad V = W*AMU1 \qquad (2.17)$$

$$\text{and} \quad T = W*AMU3 \qquad (2.18)$$

where AMU1, AMU2, and AMU3 are the constants defined by the conditions of loading.

3. Shearing stresses due to transverse shear and torque are computed for each web subpanel. The buckling interaction value, given by the buckling interaction equation [Eq.(2.9)], is then checked for each web subpanel to see if any have buckled.

4. If a subpanel has buckled, the curvature is decreased and iteration is performed to get to the theoretical buckling state of that subpanel before the value of curvature is incremented again. After buckling, a web subpanel is assumed to carry no additional normal or bending stresses beyond those present at buckling. However, additional shearing stress can develop due to the tension field action.

5. If the subpanel has not yet buckled, it is still behaving elastically. Then, the calculated load parameter represents one state of load response of the hull girder for the given value of curvature. Repeated curvature input produces an array of load parameters for the hull girder from zero to beyond the ultimate load.

Many special programming techniques were incorporated into the program. One of these deserves a detailed discussion since it considerably simplified the problems of convergence. It is presented next.

3. PROCEDURE FOR OBTAINING EQUILIBRIUM OF CROSS SECTION

3.1 Introduction

A procedure for obtaining equilibrium of the girder cross section directly for a prescribed curvature was developed as an important component of the method. The problem is to find a set of strains to meet the following requirements:

1. The value of curvature (CE) is kept constant.

2. The prescribed degree of warping (SWP) is maintained.

3. The axial force (AXF) and the bending moment about the vertical centroidal axis (YBM) are both equal to zero.

With four unknowns [the four corner strains S1, S2, S3, and S4], and the above stated independent requirements (a total of four), it should be possible to find a unique solution. However since not all of the relationships are linear, a direct solution is not possible. The procedure described next presents a method of solving this problem and it was incorporated into the computer program as subroutine TWOPLA [23].

The requirements that the degree of warping (SWP) and the value of curvature (CE) be constant, cause strains S3 and S4 to become the following functions of strains S1 and S2.

$$S3_i = S2_i + CE \left[2 - \frac{1}{SWP + 1} \right] \tag{3.1}$$

20

$$S4_i = S1_i + \frac{CE}{SWP + 1} \tag{3.2}$$

Subscript i indicates the i-th set of S1 and S2.

Once strains S3 and S4 are defined, the axial force AXF and the bending moment YBM become nonlinear functions of strains S1 and S2 only.

$$AXF = f(S1, S2) \tag{3.3}$$

$$YBM = f(S1, S2) \tag{3.4}$$

Each of these functions can be viewed as a surface with S1 and S2 being the independent variables.

The desired solution is the set of values of S1 and S2 at which both surfaces have zero values. Graphically this point can be visualized as the intersection point of the AXF and YBM surfaces and the S1-S2 plane (where AXF=YBM=0). The procedure for finding this point is an iterative procedure based on the Newton-Raphson method. In the procedure, each surface is approximated by a tangent plane defined by some three points on that surface. The

21

intersection point of these tangent planes with the S1-S2 plane gives the next approximation for the solution of S1 and S2.

Since this type of problem is encountered often in analysis of nonlinear structures, the methodology of the procedure is discussed here in considerable detail.

3.2 Methodology

The procedure for obtaining the values of S1 and S2 to make AXF and YBM equal zero for the given value of curvature starts with the assumption of the first set of $S1_1$ and $S2_1$. For example, these values could be linearly projected from a solution which was previously calculated for a lower value of curvature.

The AXF_1 and YBM_1 values computed for $S1_1$ and $S2_1$ are used as a guide for incrementing or decrementing S1 and S2 to calculate two more sets of strains and AXF and YBM. The resultant three values of AXF (AXF_1, AXF_2, and AXF_3) lie on the AXF surface and the three values of YBM on the YBM surface. In general , none of the sets of strains will give zero values of both, AXF and YBM, and a projection is made for a better set of S1 and S2. This is accomplished by using the three points on the surface to define an approximately tangent plane to each surface and solving for the set of $S1_4$ and $S2_4$ where these two planes indicate both, AXF and YBM, equal to zero as shown in Fig. 8. Then, the actual values of AXF_4 and YBM_4 are calculated for $S1_4$ and $S2_4$ and compared with the other

22

values. The process is repeated with the best three out of the four points for each plane.

Plane 1	Plane 2	
$(S1_1, S2_1, AXF_1)$	$(S1_1, S2_1, YBM_1)$	
$(S1_2, S2_2, AXF_2)$	$(S1_2, S2_2, YBM_2)$	(3.5)
$(S1_3, S2_3, AXF_3)$	$(S1_3, S2_3, YBM_3)$	

Equation (3.5) symbolically indicates the two tangent planes defined by the three initial sets of S1 and S2. Subroutine TWOPLA was written as a part of the general program to perform the projection to a better point [23]. First, subroutine TWOPLA finds the equation of each plane:

$$\text{Plane AXF:} \quad AXF_i = A1 + A2\ S1_i + A3\ S2_i \qquad (3.6)$$

$$\text{Plane YBM:} \quad YBM_i = B1 + B2\ S1_i + B3\ S2_i \qquad (3.7)$$

Coefficients (A_1, A_2, A_3) and (B_1, B_2, B_3) are computed for the fixed values of the coordinates S1, S2, AXF and YBM. In the

23

following, the methodology is shown for Plane AXF, for Plane YBM it is similar. For the AXF plane, the three linear equations of Eq. (3.6) are solved for A_1, A_2, and A_3.

$$
\begin{bmatrix} 1 & S1_1 & S2_1 \\ 1 & S1_2 & S2_2 \\ 1 & S1_3 & S2_3 \end{bmatrix} \begin{bmatrix} A1 \\ A2 \\ A3 \end{bmatrix} = \begin{bmatrix} AXF_1 \\ AXF_2 \\ AXF_3 \end{bmatrix} \tag{3.8}
$$

Using the terminology of Cramer's Rule (solution by determinants)

$$
A1 = \frac{D1}{D} \tag{3.9}
$$

$$
A2 = \frac{D2}{D} \tag{3.10}
$$

$$
A3 = \frac{D3}{D} \tag{3.11}
$$

where D1, D2, D3 are the numerator determinants and D is the determinant of the coefficient matrix.

Substitution of Eqs. (3.9),(3.10) and (3.11) into Eq. (3.6) yields Eq. (3.12) for the AXF-plane.

24

$$D*AXF = D1 + D2 \; S1 + D3 \; S2 \qquad\qquad (3.12)$$

An analogous procedure for the YBM-plane results in

$$E*YBM = E1 + E2 \; S1 + E3 \; S2 \qquad\qquad (3.13)$$

where E, E1, E2 and E3 correspond to D, D1, D2 and D3 of the AXF-plane, respectively.

In both of these equations [Eqs.(3.12), (3.13)], S1 and S2 are free variables. To find their values where both planes give a zero function, Eqs.(3.14) and (3.15) are solved simultaneously for the fourth set of S1 and S2, i.e., $S1_4$ and $S2_4$.

$$D1 + D2 \; S1 + D3 \; S2 = 0 \qquad\qquad (3.14)$$

$$E1 + E2 \; S1 + E3 \; S2 = 0 \qquad\qquad (3.15)$$

Since the AXF and YBM surfaces are generally curved, not plane, the values of AXF_4 and YBM_4 calculated for these strains will not be equal to zero. By replacing the worst point of each plane with the new values and repeating the procedure, a set of

25

strains S1 and S2 is found which causes both, AXF and YBM to be equal to zero within a prescribed tolerance. Figure 8 shows the AXF and YBM planes for some later iteration , when each is defined by a separate set of three points. Their intersection point on the S1-S2 plane gives the next approximation for S1 and S2.

To accelerate convergence, it was found that the two dependent functions, AXF and YBM, should be of approximately the same order of magnitude. To achieve this, the values of YBM are divided by a constant before they are entered into subroutine TWOPLA. This constant is related to the first-yield moment about the vertical axis.

3.3 Limitations of the Procedure

Most of the time, subroutine TWOPLA performed very well (3-4 iterations). However, there are some cases that require special treatment, these are: (1) both planes are parallel to each other; (2) one or both planes are perpendicular to the S1-S2 plane; (3) the intersection line of the two planes is parallel to the S1-S2 plane; (4) one or both planes are coincident with the S1-S2 plane.

Solution of these special cases is planned as an improvement of the program; at present, a corresponding message is printed.

4. WARPING OF CROSS SECTION

4.1 General

Test observations have shown the possibility of warping of the girder cross section , that is, of non-planar distribution of strains. To include this effect in the proposed method of analysis, the degree of warping was defined in terms of the mid-width curvature by

$$SWP = \frac{\Delta S3}{2(S4-S1)} \qquad (4.1)$$

where S1 and S4 are the strains at the top and bottom of Web 1 of the cross section as shown in Figs. 9 and 3, and $\Delta S3$ is the increase (or decrease) of strain S3 relative to the value of S3 as would be given by the plane defined by the strains at the other three corners (S1, S2, S4).

The effect of warping was introduced into the computational procedure as described in the preceeding chapter. A specific study of the effect of warping was conducted for Lehigh Test 3 [21] which was subjected to the combined action of bending, shear and torque (other results of this test are described in Chapter 5). Two aspects were looked into: (1) the effect of warping at low and high levels of loading, that is, respectively, when there was no buckling in the web subpanel, and after some web subpanels have buckled in the heavier loaded web, Web 1; and (2) a procedure for

determining the optimum degree of warping which would most likely develop in the girder segment.

4.2 Effect of Warping at Low and High Loads

In Figure 10(b), load parameter W is non-dimensionalized with respect to W_o which is the load parameter for zero degree of warping. The W/W_o is plotted against the degree of warping SWP varying from -0.5 to +0.5 while the curvature is kept constant.

The dashed curve in Fig. 10(b) is for a low value of curvature when there is no buckling in the web subpanels at zero warping. The .essentially horizontal curve indicates that warping had no influence on the load parameter. Only at a rather high negative warping of SWP = -0.4 there begins a reduction of W/W_o due to the buckling in the web at this large distortion.

The solid curve in Fig. 10(b) is for a larger value of curvature, almost at the ultimate load. Some web subpanels have already buckled and the nonlinear effect of the degree of warping is quite pronounced. The curve is somewhat irregular due to the tolerance limitations in various iterative routines in the computer program, but the scatter is quite small, less than 1%.

Thus, it can be concluded that warping becomes a noticeable influence only at higher levels of loading, after the behavior of some of the girder section components become nonlinear due to

buckling or other effects. Before that, the effective section remains symmetric and is not influenced by warping.

4.3 Optimum Degree of Warping

The solid curve of Fig. 10(b) is replotted in Fig. 10(a) but with respect to the actual value of the load parameter W which was the load applied to the test specimen. After smoothening (averaging) the curve as shown in the figure by the dashed curve, one can see that there is a maximum value of the load parameter W approximately at the degree of warping of SWP = +0.1.

These plots indicate a plausible procedure for determining the optimum value of the degree of warping. A series of W values should be computed for a constant value of curvature by varying the degree of warping SWP from a small negative value, say SWP = -0.2, to a small positive value, such as, SWP = +0.3 (four to six points, including a point at SWP = 0.0 for the plane section). Then, a parabolic curve can be used to smoothen the computed points and to determine the maximum value of W_{max}, as well as the W_o value at zero warping.

The study illustrated in Fig. 10(a) seems to indicate that the assumption of a planar section (zero warping) should introduce only a small error. This appears to be reasonable as long as the cross section behaves as a closed section without a shift of the shear

29

center.   Consequently, this procedure was not incorporated into the

computer program.

5. COMPARISON OF THEORETICAL AND EXPERIMENTAL RESULTS

In order to verify the accuracy of the proposed method, theoretical and experimental results are compared in Tables 2 and 3 for the available twelve tests. Included are tests on box sections subjected to pure moment, to moment combined with shear or to moment, shear and torque. The only tests that appear to be available are those conducted at Lehigh University [17, 21], the Imperial College of London [5] and one test by Reckling [4]. In the following, the principal characteristics of each test are described and the theoretical and experimental results are compared. Explanation is given for any special methods or observations which may contribute to the understanding of any discrepancies. First are described the tests at Lehigh University as a group, then the tests conducted at the Imperial College and, lastly, the test reported by Reckling.

5.1 Lehigh Tests

5.1.1 Description of Specimen and Tests

The scantlings of the test specimen were selected to model portions of a typical hull girder, and the relative proportions of each component were approximately the same as used in engineering practice. The scantings of each test segment (the portion of the girder between adjacent transverse stiffeners) were: length

31

- 457.2mm (18 in.), width - 667mm (26.25 in.), depth - 508mm (20 in.), and plate thickness - 1.85mm (0.072 in.). There were two equally spaced longitudinal stiffeners on each web and five equally spaced stiffeners on each flange. All of them were 19.0 mm (0.748 in) wide and 3.2 mm (0.126 in) thick. The yield stress of the specimen was 238 MPa (34.34 ksi).

Figure 11 shows the test specimen which was designed for the purpose of conducting three tests. For each test, a particular segment was tested to failure while the adjoining segment(s) were reinforced. The three identical segments were each subjected to different combinations of moment, shear and torque which are listed in the figure to the right of the sketches.

For Test 1, the adjacent segment, Segment 2, was temporarily reinforced by using: (1) small steel bars "C"-clamped to the longitudinal stiffeners, (2) corner angles at the web to compression flange junctions, and (3) pieces of wood on the compression flange. All of these reinforcements were tightly wedged between the transverse stiffeners. Their function was to reduce the axial force in the compression flange of Segment 2.

For Test 2, the segment which failed in Test 1 was permanently reinforced with four steel bars and two corner angles tack welded to the compression flange and wedged between transverse stiffeners. The webs were reinforced with steel bars placed in the direction of

the tension diagonals. All of these reinforcements were welded to the transverse stiffeners. Meanwhile, the segment reserved for Test 3 was reinforced by steel bars clamped to the longitudinal stiffeners and pieces of wood wedged between transverse stiffeners.

For Test 3, the failed segment of Test 2 was permanently reinforced in the manner of Segment 1.

5.1.2 General Observations

Measurement of initial imperfections of the plate components showed that the out-of-flatness of the compression flange was 2 to 3 times the plate thickness. These high imperfections were caused by the welding process during fabrication. Although not measured, the residual stresses were expected to be relatively high. Additional initial imperfections were created in Segment 2 as a consequence of Test 1 and in Segment 3 after Tests 1 and 2.

The reinforcing system used during testing created some undesirable effects which became especially evident for Test 2. The compression flange of this segment buckled downward (convex on the plate side) instead of upward, as was expected. The reason for this behavior was an apparent upward shift of the centroid of the cross section at one end of the segment due to the reinforcements of Segment 3, and due to a negative residual moment (causing compression in the stiffeners) introduced by the process of wedging. At the other end of Segment 2 adjoining Segment 1, there

33

was a similar upward shift of the centroid and a moment which remained from the plastification of the longitudinals in Test 1. The net result was that the compression flange was subjected to residual flexure which in combination with the applied loads forced the flange to deflect downward, rather than upward, as would have been expected.

The eccentricity of the vertical load on the specimen changed somewhat during the course of Tests 2 and 3. This was due to the angle of rotation of the girder, as well as, to the distortion of the shape of the cross section in the latter stages of the tests and the consequent lateral shift of the compression flange. Although adjustments of the point of load application were made during the test, the eccentricity could not be kept constant continuously.

During Test 2, there was also a noticeable change of the shape of the cross section, especially, of the end transverse frame which resisted the torque. For Test 3, this end frame was braced by a diagonal bar to prevent this type of distortion.

In consequence of all of the detrimental complications associated with these tests, the experimental results were expected to be on the low side, especially, for the tests with torque (Tests 2 and 3) when compared with the results which would have been expected for more ideal test specimens.

5.1.3 Lehigh - Test 1 (Moment and Shear)

The theoretical ultimate strength of the segment for Test 1 was 1.8% below the experimental ultimate strength as shown in Fig. 12 and Table 2. The ultimate strength of the section was limited by the strength of the compression flange. Considering the condition of the test specimen, this correlation was much better than could have been expected.

5.1.4 Lehigh - Test 2 (Moment, Shear, and Torque)

The experimental ultimate strength of Segment 2 was expected to be greater than the experimental ultimate strength of Segment 3 since both segments were geometrically identical and the loading was nearly the same except that Segment 3 was subjected to a somewhat greater amount of torque and shear.

However, the theoretical ultimate strength was 49.1% over the experimental strength as shown in Fig. 13 and Table 2. This exceptionally low experimental ultimate strength of Test 2, can be attributed to the effects which caused the compression flange to buckle downward, instead of upward as discussed above in Subsection 5.1.2.

35

5.1.5 Lehigh - Test 3 (Moment, Shear, and Torque)

The theoretical ultimate strength of the girder for this test was 26.4% greater than the experimental ultimate strength as shown in Fig 14 and Table 2. In view of the many factors which detrimentally influenced this test (see Subsection 5.1.2), the agreement is not as bad as could have been expected.

5.2 Imperial College and Reckling Tests

Eight tests performed by Dowling at the Imperial College [5] and one by Reckling [4] are compared next with the theory. Among these, only one test included torsion.

5.2.1 Imperial College - Model 1 (Moment and Shear)

The scantlings of the test segments in the specimen were: length - 787.44mm (31 in.), width - 1219.2mm (48 in.), depth - 914.4mm (36 in.), flange plate thickness - 4.95mm (0.195 in.), and web plate thickness - 3.38mm (0.133 in.). There were four equally spaced stiffeners on each flange and two stiffeners on each web. The flange and web plates of the specimen had the yield stresses of 247 MPa (35.8 ksi) and 273 MPa (39.7 ksi), respectively.

The theoretical ultimate strength was 9.8% greater than the experimental ultimate strength, as shown in Fig. 15 and listed in Table 2. The ultimate strength of the model was limited by the

capacity of the compression flange.

5.2.2 Imperial College - Model 2 (Moment)

The scantlings of the test segments were: length - 787.4mm (31 in.), width - 1219.2mm (48 in.), depth - 914.4mm (36 in.), flange plate thickness - 4.88mm (0.192 in.), and web plate thickness - 3.38mm (0.133 in.). There were four equally spaced stiffeners on each flange and two stiffeners on each web. The yield stresses of the flange and web plates were 298 MPa (43.2 ksi) and 212 MPa (30.7 ksi), respectively.

The theoretical ultimate strength was 9.2% greater than the experimental ultimate strength (Fig. 16 and Table 3). The strength of the girder was limited by the ultimate strength of the compression flange.

5.2.3 Imperial College - Model 3 (Moment and Shear)

The scantlings of the test specimen were: length - 787.4mm (31 in.), width - 1219.2mm (48 in.), depth - 914.4mm (36 in.), compression flange thickness - 5.02mm (0.198 in.), tension flange plate thickness - 4.95mm (0.195 in.), and web plate thickness - 4.98mm (0.191 in.). There were nine equally spaced stiffeners on each flange and five stiffeners on each web. The compression and tension flange plates had the yield stresses of 221 MPa (32.0 ksi) and 216 MPa (31.2 ksi), respectively. The yield stress of the web

37

plates was 281 MPa (40.8 ksi).

The theoretical ultimate strength was 3.2% greater than the experimental ultimate strength, as shown in Fig. 17 and Table 2. The ultimate strength of the model was limited by the capacity of the compression flange.

5.2.4 Imperial College - Model 4 (Moment)

The scantlings of this test specimen were: length - 787.4mm (31 in.), width - 1219.2mm (48 in.), depth - 914.4mm (36 in.), compression flange plate thickness - 5.03mm (0.198 in.), tension flange plate thickness - 4.95mm (0.195 in.), and web plate thickness - 4.98mm (0.196 in.). The yield stresses of the compression and tension flange plates were 221 MPa (32.0 ksi) and 216 MPa (31.4 ksi), respectively. The yield stress of the web plate was 281 MPa (40.8 ksi). There were nine equally spaced stiffeners on each flange and four stiffeners on each web.

The theoretical ultimate strength was 4.8% below the experimental strength as shown in Fig. 18 and Table 3. The ultimate strength was limited by the capacity of the compression flange.

5.2.5 Imperial College - Model 5 (Moment and Shear)

The scantlings of the test specimen were: length - 787.4mm (31 in.), width - 1219.2mm (48 in.), depth - 914.4mm(36 in.), flange plate thickness - 8.128mm(0.320 in.), and web plate thickness - 3.15mm (0.124 in.). There were four equally spaced stiffeners on each flange and two stiffeners on each web. The flange and web plates of the specimen had the yield stresses of 264 MPa (38.3 ksi) and 233 MPa (33.8 ksi), respectively.

The computed ultimate strength was 57.3% greater than the experimental as shown in Fig. 19 and Table 2. According to the method, the ultimate strength was limited by the shear capacity of the webs on the assumption that the longitudinal stiffeners did not buckle. However, the photographs of Model 5 in the source publication [5] showed that all of the web longitudinal stiffeners had buckled before the ultimate load was reached. To take this into account the model was analyzed again, this time assuming the web to be without stiffeners. The theoretical prediction become significantly closer to the test result; only 22.6% above the experimental strength.

5.2.5 Imperial College - Model 5 (Moment and Shear)

The scantlings of the test specimen were: length - 787.4mm (31 in.), width - 1219.2mm (48 in.), depth - 914.4mm(36 in.), flange plate thickness - 8.128mm(0.320 in.), and web plate thickness - 3.15mm (0.124 in.). There were four equally spaced stiffeners on each flange and two stiffeners on each web. The flange and web plates of the specimen had the yield stresses of 264 MPa (38.3 ksi) and 233 MPa (33.8 ksi), respectively.

The computed ultimate strength was 57.3% greater than the experimental as shown in Fig. 19 and Table 2. According to the method, the ultimate strength was limited by the shear capacity of the webs on the assumption that the longitudinal stiffeners did not buckle. However, the photographs of Model 5 in the source publication [5] showed that all of the web longitudinal stiffeners had buckled before the ultimate load was reached. To take this into account the model was analyzed again, this time assuming the web to be without stiffeners. The theoretical prediction become significantly closer to the test result; only 22.6% above the experimental strength.

5.2.6 Imperial College - Model 6 (Moment and Shear)

The scantlings of the test specimen were: length - 787.4mm (31 in.), width - 1219.2mm (48 in.), depth - 1219.2mm (48 in.), compression flange thickness - 4.8mm (0.192 in.), web plate thickness - 3.35mm (0.132 in.), tension flange thickness - 6.25mm (0.246 in.), and tension flange coverplate - 813mm (32 in.) by 37.6mm (1.48 in.). There were nine longitudinal stiffeners on the compression flange and seven on each web. The plate of the compression flange and web had yield stress of 271 MPa (39.4 ksi) and 315 MPa (45.7 ksi), respectively.

The theoretical ultimate strength was 9.5% over the experimental as shown in Fig. 20 and Table 2. Theoretically, the shear capacity of the webs controlled the strength.

5.2.7 Imperial College - Model 7 (Moment, Shear, and Torsion)

This is the only specimen in this series which was subjected to torsion in addition to shear and moment. The scantlings of the test specimen were: length - 787.4mm (31 in.), width - 1219.2mm (48 in.), depth - 914.4mm (36 in.), compression flange plate thickness - 7.80mm (0.307 in.), tension flange plate thickness - 7.95mm (0.313 in.), and web plate thickness - 3.15mm (0.124 in.). There were four stiffeners on each flange and two on each web. The compression flange and web plates of the specimen had the yield stress of 273 MPa (39.6 ksi) and of 236 MPa (34.3 ksi),

40

respectively.

The computed ultimate strength was 51.6% greater than the experimental (Fig. 21 and Table 2). The ultimate strength was indicated to be limited by the shear capacity of the web which was subjected to the higher shear stress (due to torsion). However, similarly to Model 6, the test photographs indicate occurence of buckling of the web stiffeners before the ultimate load was reached. A re-analysis of the specimen with the web stiffeners assumed to be removed brought the theoretical capacity to only 8.9% above the test strength.

5.2.8 Imperial College - Model 8 (Moment and Shear)

The test on Model 8 is included here although its compression flange failed in a grillage mode, that is, combined failure of the longitudinals and transverses, which is not considered by the proposed method of analysis. The scantlings of the specimen were the following: length - 1320.8mm (52 in.), width - 1219.2mm (48 in.), depth - 914.4mm (36 in.), compression flange plate thickness - 4.72mm (0.186 in.), tension flange plate thickness - 4.67mm (0.184 in.), and web plate thickness - 3.18mm (0.125 in.). There were nine stiffeners on each flange and four on each web. The yield stress of the compression and tension flange plates were 276 MPa (40.1 ksi) and 365 MPa (53.1 ksi) respectively, and the yield stress of the web was 252 MPa (36.5 ksi).

41

The theoretical ultimate strength was 46.5% greater than the test strength as indicated in Fig. 22 and Table 3. Since the ultimate strength of this model was observed to be limited by the overall buckling of the compression flange, including the transverses, the overestimate is not surprising. This test indicates the need to extend the method to include the grillage mode to cover the girders with weak transverses.

5.2.9 Reckling - Test 23 (Moment)

Only nominal design dimensions of this test specimen were reported in the publication [4]: length - 500mm (19.68 in.), width - 600mm (23.62 in.), depth - 400mm (15.75 in.), and plate thickness - 2.5mm (0.098 in.). The reported nominal yield stress of this model was 246 MPa (35.7 ksi).

The theoretical ultimate strength was 6.0% lower than the experimental (Fig. 23 and Table 3). The theoretical strength was limited by the ultimate strength of the compression flange.

The validity of the comparison for this test is somewhat questionable because only nominal design values for dimensions and material properties were available rather than the measured. Since generally, the actual values tend to be somewhat greater than nominal, the slight underestimate of the capacity is quite reasonable.

42

6. SUMMARY, CONCLUSIONS AND RECOMMENDATIONS

6.1 Summary and Conclusions

A number of methods have been proposed which rationally compute the ultimate bending strength of ship hull girders, and one of these methods gives a relatively good correlation with test results. However, none of them has provisions for considering the effects of shear and, especially, torque in addition to bending.

A new method is presented here for determining the behavior and ultimate strength of longitudinally stiffened ship hull girders subjected to moment, torque and shear. For the geometry and material properties of a segment between transverse stiffeners of the ship hull, the method gives a relationship between the curvature and a load parameter. This load parameter defines the values of moment, torque and shear acting on the cross section. The principal features of this analytical method are: (1) compatibility of axial strains is maintained, by keeping the cross section plane or subjecting it to a specified degree of warping; (2) compatibility of shearing strains in each web is maintained; (3) non-linear behavior of individual components due to buckling, large deflections, residual stresses and plastification is taken into account.

Some of the important assumptions used in this method are the following:

43

1. The segment is prismatic and the shape of the cross section does not change.

2. The nonlinear axial behavior of the compression flange elements (stiffener-plate combinations) must be pre-defined by a series of points which are provided by other computer programs which consider nonlinear behavior due to plate buckling, initial imperfections, residual stresses, and the beam-column effect.

3. The axial behavior of the tension flange is of an elastic-plastic pattern with the plastic limit determined by yielding due to shearing and axial stresses.

4. The axial behavior of the web plate subpanels is elastic-plastic with the plastic limit determined by the buckling interaction equation or yielding. The shear response is defined by an ultimate strength theory previously developed for longitudinally stiffened plate girders which considers tension-field action in web subpanels.

5. The stiffeners of the web and tension flange are elastic-plastic.

6. The effect of shear lag is negligible.

The basic procedure of the method is to compute the forces in the cross section (moment, torque and shear) for a prescribed curvature and a constant degree of warping, increment the

44

curvature, and repeat the process. Thus, for a specific value of curvature a set of four axial strains, one at each corner, is found. This set of strains must satisfy requirements of equilibrium, that is, the total axial force and the moment about the vertical axis are each equal to zero. With the axial strain distribution known, the bending moment can be calculated and, because the relative amounts of shear, moment, and torque are prescribed, the corresponding values of torque and shear are computed from the moment. The shearing stresses, due to flexure and torsion, are determined in the cross section, and each component is checked for the conditions of buckling and/or yielding. If the condition is exceeded, the curvature is reduced and the process repeated to convergence. Then, the curvature is incremented for the next point. As part of the computational process, a new efficient technique for enforcing equilibrium of forces in the cross section was employed.

A comparison of the theoretical and experimental results for tests on twelve specimens subjected to various combinations of moment, shear and torque showed the method to be acceptably accurate (within 10%) for the specimens which satisfy the assumptions of the method, that is, maintain their cross-sectional shape, have web stiffeners which do not buckle, and have "rigid" transverses. The greater deviations for the four specimens which

did not satisfy these requirements could be readily explained and/or adjusted. The accuracy of the method, thus, can be considered to be confirmed by the available experimental results.

The following additional studies and observations were made during this research:

1. A study of the sensitivity of a girder segment to warping of the cross section indicated that warping was insignificant for the cross sections which were analyzed; hence, an assumption of "a plane section remains plane" should be adequate for "usual" sections.

2. The assumption of the method that the effects of shear lag are negligible was confirmed by observing the almost linear distribution of strains in the tension flanges of the test specimens for which data were available.

3. One of the specimens (Dowling - M8) included in the comparison had its capacity limited by the grillage mode failure of the compression flange (overall failure of the longitudinal and transverse stiffeners). This failure mode is not considered in the proposed method and the prediction was significantly higher than the test result.

6.2 Recommendations for Future Research

On the basis of the conducted work, the following topics are recommended for future research for the purpose of improving the proposed method or for extending knowledge of the structural behavior of box girders:

1. Axial strength and behavior of longitudinal web stiffeners, specifically, proper evaluation of the forces in the stiffeners due to the effects of bending and tension-field action.

2. Effect of shearing stresses on the axial behavior of the compression flange and on its components.

3. Grillage mode of behavior for compression flange, that is, when the transverses cannot be assumed to be rigid.

4. Effect of different degrees of modification on the response of the cross-sectional components due to torque, on the stress distribution and on the overall behavior of the segment (shifting of the shear center).

5. More tests on ship hull models subjected to moment, torque and shear. (At present, only three test results are available and none of them properly duplicate prototype conditions.)

7. NOMENCLATURE

a	Length of girder segment.
$A1, A2, A3$	Coefficients in the equation of the AXF-Plane; Equation (3.6).
A_o	Enclosed area of the cross section.
A	Aspect ratio.
A_i	Aspect ratio of the i-th subpanel.
A_{min}	Aspect ratio of the widest web subpanel.
AMU1	Coefficient that relates shear force in the section to the load parameter.
AMU2	Coefficient which relates moment in the section to the load parameter.
AMU3	Coefficient which relates torque in the section to the load parameter.
AXF	Axial force in the hull girder.
$B1, B2, B3$	Coefficients in the equation of the YBM-Plane; Equation (3.7).
b	Width of the hull girder.
CE	Curvature at mid-width of the hull girder.
d	Depth of the hull girder.
d_i	Depth of the i-th web subpanel.
$d_{i\ max}$	Largest subpanel depth.
E	Modulus of elasticity.
F_{bcri}	Critical bending buckling stress of the i-th web subpanel for the case of bending acting alone.

F_{ccri} Critical compressive buckling stress for the i-th web subpanel for the case of axial compression acting alone.

F_{vcri} Critical shear buckling stress of the i-th web subpanel for the case of shear acting alone.

F_y Yield stress.

G Shearing modulus.

q_t Shear flow.

r Shear strain.

r_{cri} Shear strain in the i-th web subpanel at the point of buckling.

r_{ui} Shear strain in the i-th web subpanel when it first reaches its ultimate shear strength.

S_{bcri} Bending stress which causes buckling of the i-th web subpanel when acting simultaneously with S_{ccri} and $_{vcri}$.

S_{ccri} Compressive stress which causes buckling of the i-th web subpanel when acting simultaneously with S_{bcri} and $_{vcri}$.

S_{ti} Tension field stress at the ultimate condition for the i-th web subpanel.

$S_{t\ max}$ Normal stress which causes yielding of the tension flange when acting simultaneously with shear.

$S1,S2,S3,S4$ Axial strain at the corners of the girder(see Fig. 2).

$\Delta S3$ See Fig. 9.

SWP Degree of warping, see Fig. 9.

     Shear stress.

τ_{tfi} Equivalent shearing stress in the i-th web subpanel.

τ_{vcri} — Shearing stress which causes buckling of the i-th web subpanel when acting simultaneously with S_{bcri} and S_{ccri}.

T — Torque.

t_w — Web thickness.

V — Total shear force carried by both webs.

V_{bi} — Shear force present at buckling of the i-th web subpanel.

V_{ft} — Shear force in each flange due to torque.

V_{tfi} — Shear force carried by tension field action in the i-th subpanel.

V_{wt} — Shear force in each web due to torque.

W — Load parameter.

W_o — Load parameter for SWP = 0 (plane section).

YBM — Resultant bending moment about the vertical centroidal axis of the hull girder.

TABLES

51

Table 1   Reference Buckling Stresses
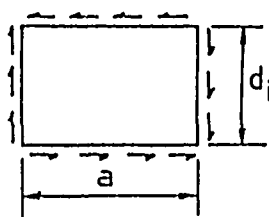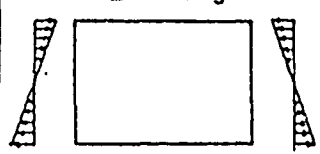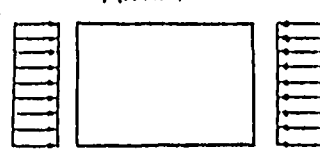
Pure Stress	Aspect Ratio $\alpha = a/d_i$	Buckling Coefficient k	Relative Plate Slenderness	For λ	Buckling Stress / Yield Stress
Shear		$k_v = 5 + \dfrac{5}{\alpha^2}$	$\lambda_v = 0.8 \dfrac{d_i}{t_w}\sqrt{\dfrac{F_y}{E\,k_v}}$	≤ 0.58	$\dfrac{F_{vcr}}{F_y} = 0.58$
				≥ 0.58 ≤ 1.41	$\dfrac{F_{vcr}}{F_y} = 0.58 - 0.357(\lambda_v - 0.58)^{1.18}$
				> 1.41	$\dfrac{F_{vcr}}{F_y} = 0.58(1/\lambda_v^2)$
Bending	$> \dfrac{2}{3}$	$k_b = 24$	$\lambda_b = \dfrac{d_i/t_w}{0.95}\sqrt{\dfrac{F_y}{E\,k_b}}$	≥ 0.65 ≤ 1.5	$\dfrac{F_{bcr}}{F_y} = 0.072(\lambda_b - 5.62)^2 - 0.78$
	$< \dfrac{2}{3}$	$k_b = 24 + 73(\dfrac{2}{3} - \alpha)^2$		≥ 1.5	$\dfrac{F_{bcr}}{F_y} = 1/\lambda_b^2$
Axial	> 1	$k_c = 4$	$\lambda_c = \dfrac{d_i/t_w}{0.95}\sqrt{\dfrac{F_y}{E\,k_c}}$	≥ 0.65 ≤ 1.5	$\dfrac{F_{ccr}}{F_y} = 0.072(\lambda_c - 5.62)^2 - 0.78$
	< 1	$k_c = (\alpha + \dfrac{1}{\alpha})^2$		≥ 1.5	$\dfrac{F_{ccr}}{F_y} = 1/\lambda_c^2$

Table 2   Comparison of Theoretical and Experimental Results
Tests for (Moment and Shear) and
(Moment, Shear, and Torque)

TEST NUMBER	LOADING[*]			ULTIMATE LOAD (kN)		$\frac{W_{th}-W_{exp}}{W_{exp}}$ (%)
	$\frac{V}{W}$	$\frac{M}{Vd}$	$\frac{T}{Vd}$	W_{exp}	W_{th}	
Ref.[17] T1	0.615	1.799	0	266.9	262.0	-1.8
T2	0.385	3.150	0.990	164.6	245.4	49.1
Ref.[27] T3	0.538	2.252	0.732	192.4	243.1	26.4
Ref.[5] M1	0.500	2.153	0	1315.2	1444.3	9.8
M3	0.500	2.153	0	1913.0	1975.9	3.2
M5	0.500	2.153	0	1115.9	1367.9	22.6
M6	0.500	1.615	0	2650.3	2902.3	9.5
M7	0.500	2.153	0.583	817.0	890.3	8.9

[*] W = Load
V = Flexural shear
M = Moment
T = Torque
d = Depth of section

Table 3   Comparison of Theoretical and Experimental Results
Tests for Pure Moment

TEST NUMBER	ULTIMATE LOAD (kN) W_{exp}	ULTIMATE MOMENT (kN-m)		$\dfrac{M_{th}-M_{exp}}{M_{exp}}$ (%)
		M_{exp}	M_{th}	
Ref.[5] M2	642.6	1542.2	1684.6	9.2
M4	896.7	2152.1	2048.9	-4.8
M8	553.0	1327.2	1944.2	46.5
Ref.[4] R23	-----	237.8	223.5	-6.0

FIGURES
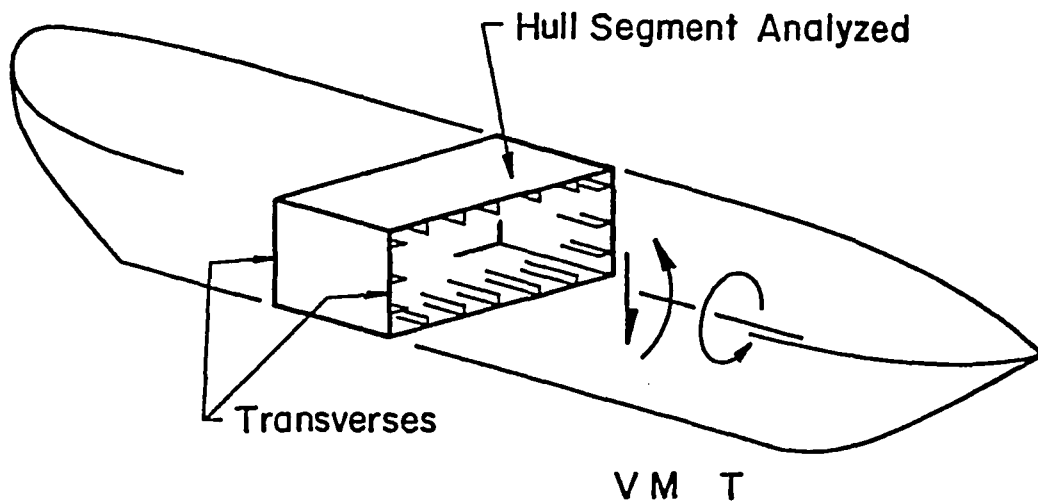
Fig.1   Segment of Hull Girder Subjected to Bending (M),
        Torque (T), and Shear (V)

56
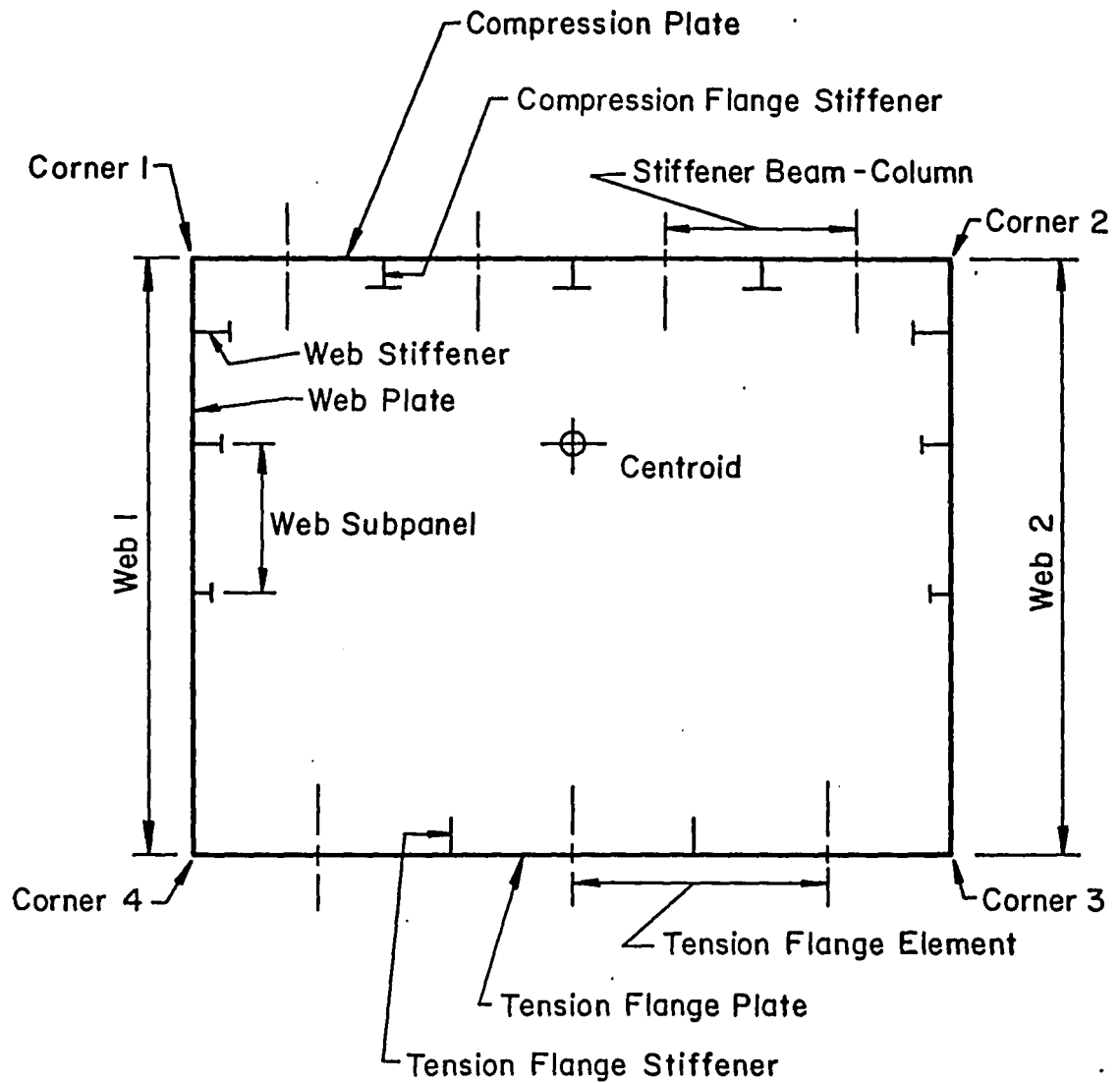
Fig.2 Definition of Components in a Cross Section
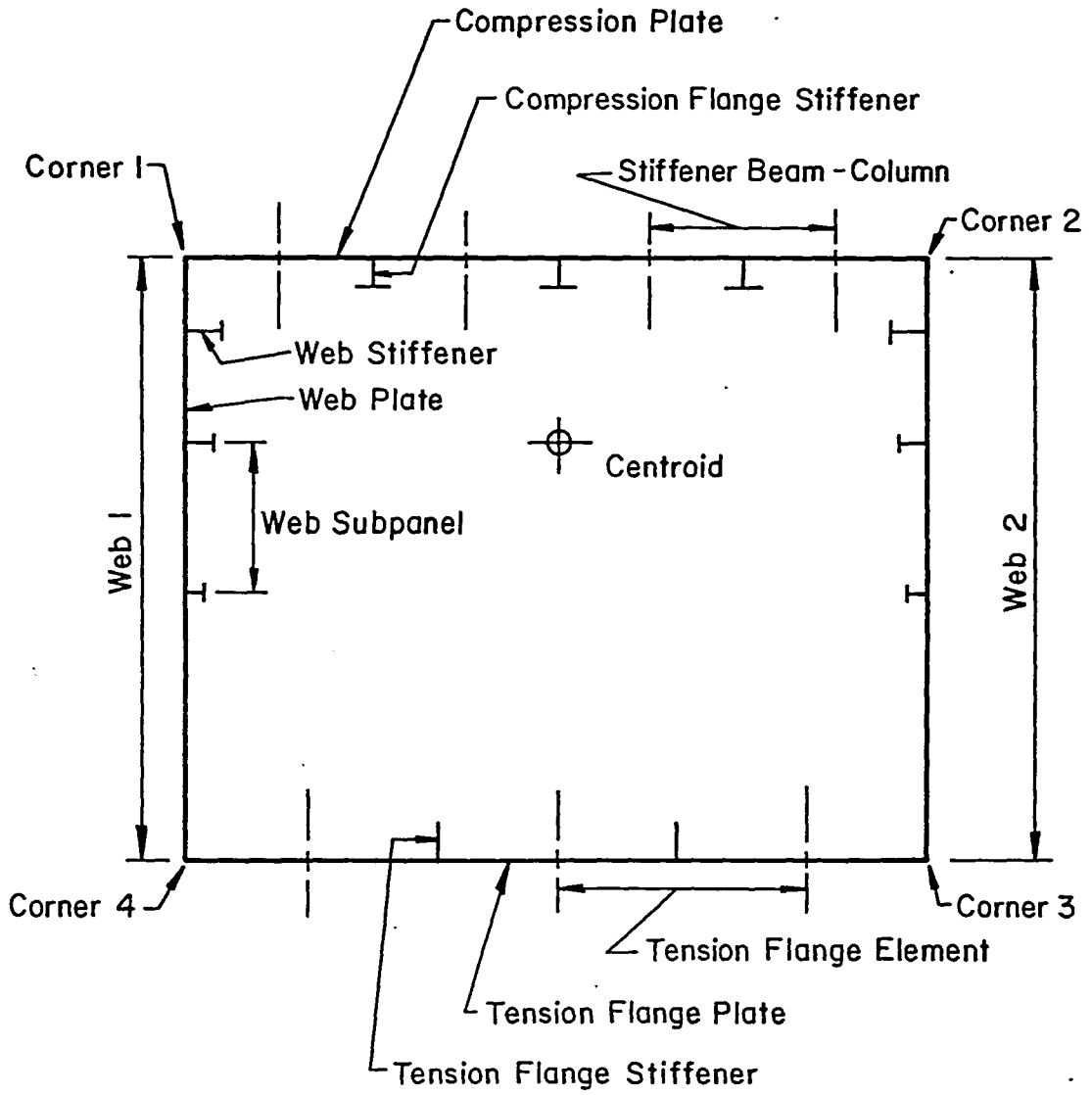
Fig.2 Definition of Components in a Cross Section
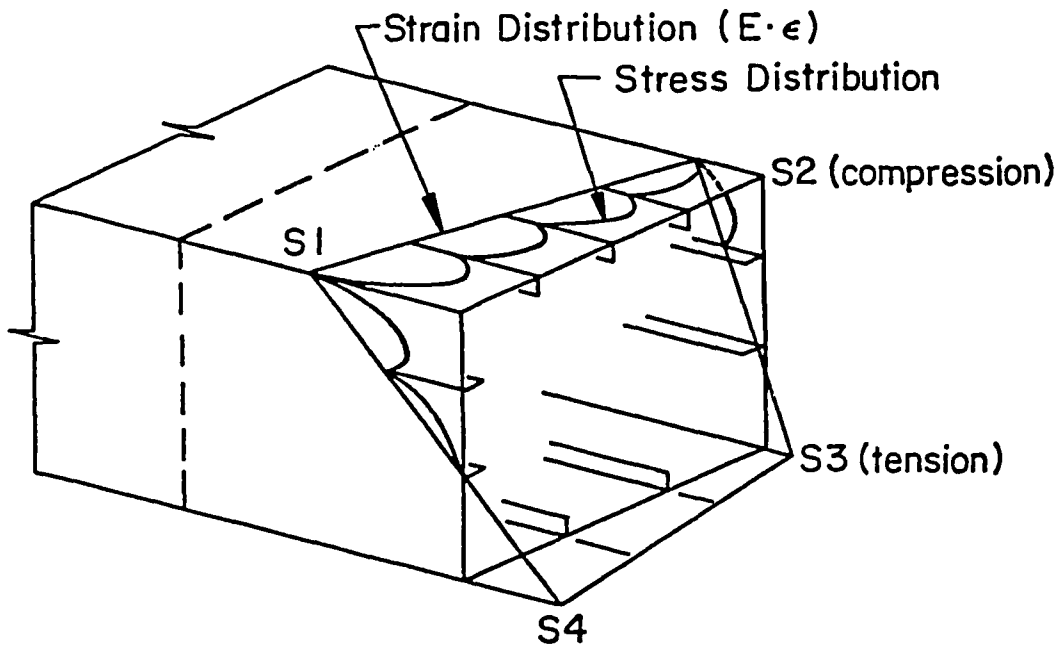
Fig.3 Stress and Strain Distributions in Girder Cross Section
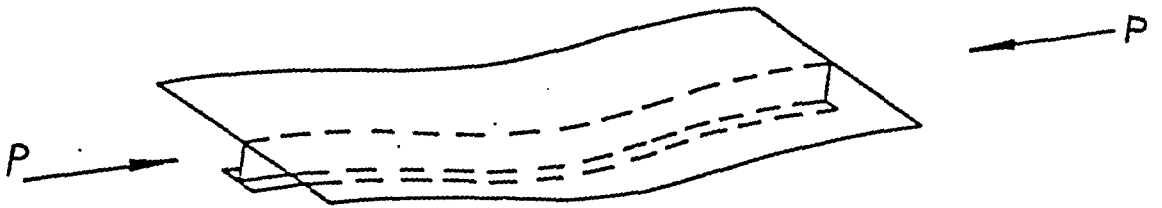
Fig.4 Compression Flange Beam-Column
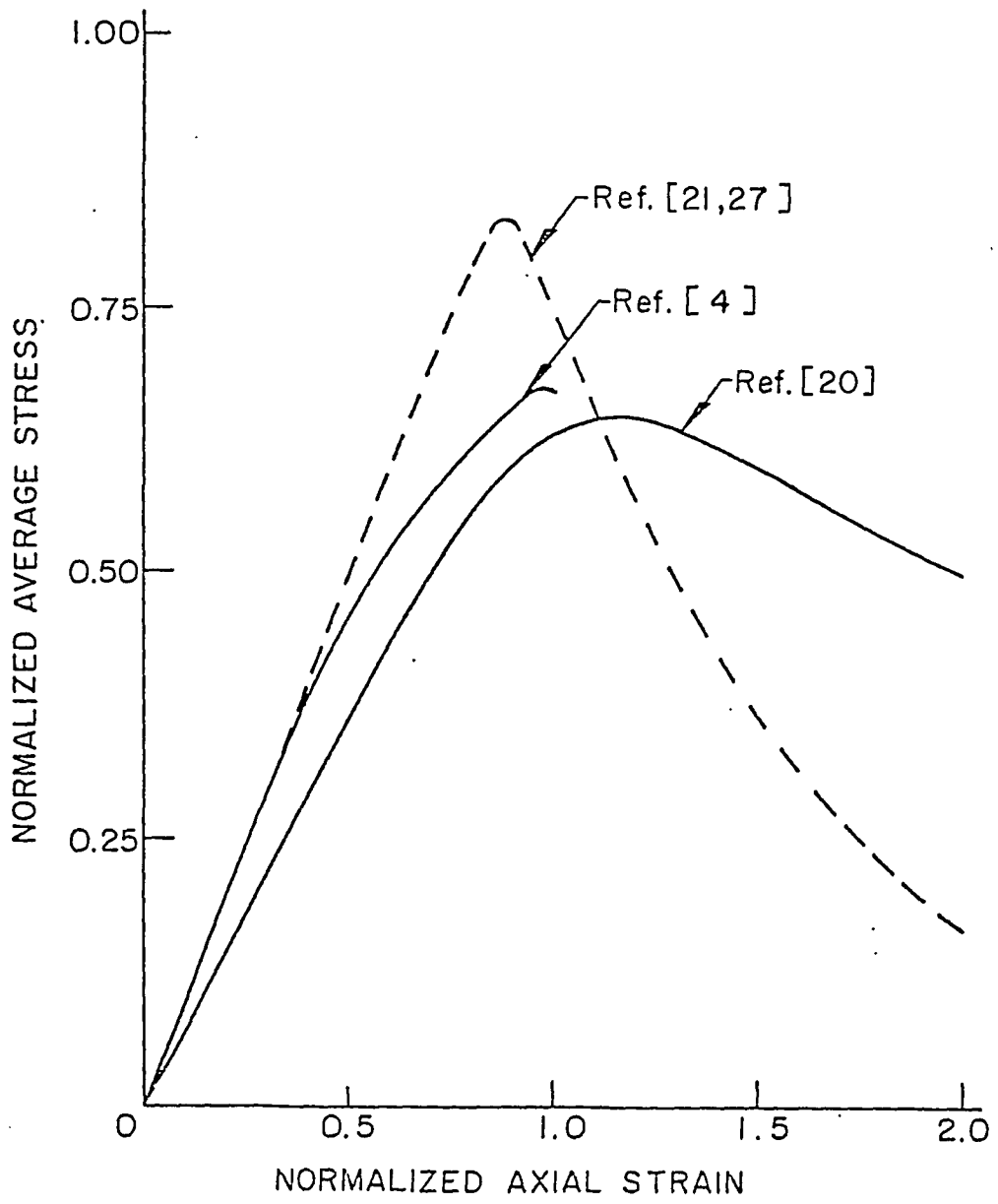
Fig.5 Load Response of Compression Flange for Lehigh Specimen
by Three Methods
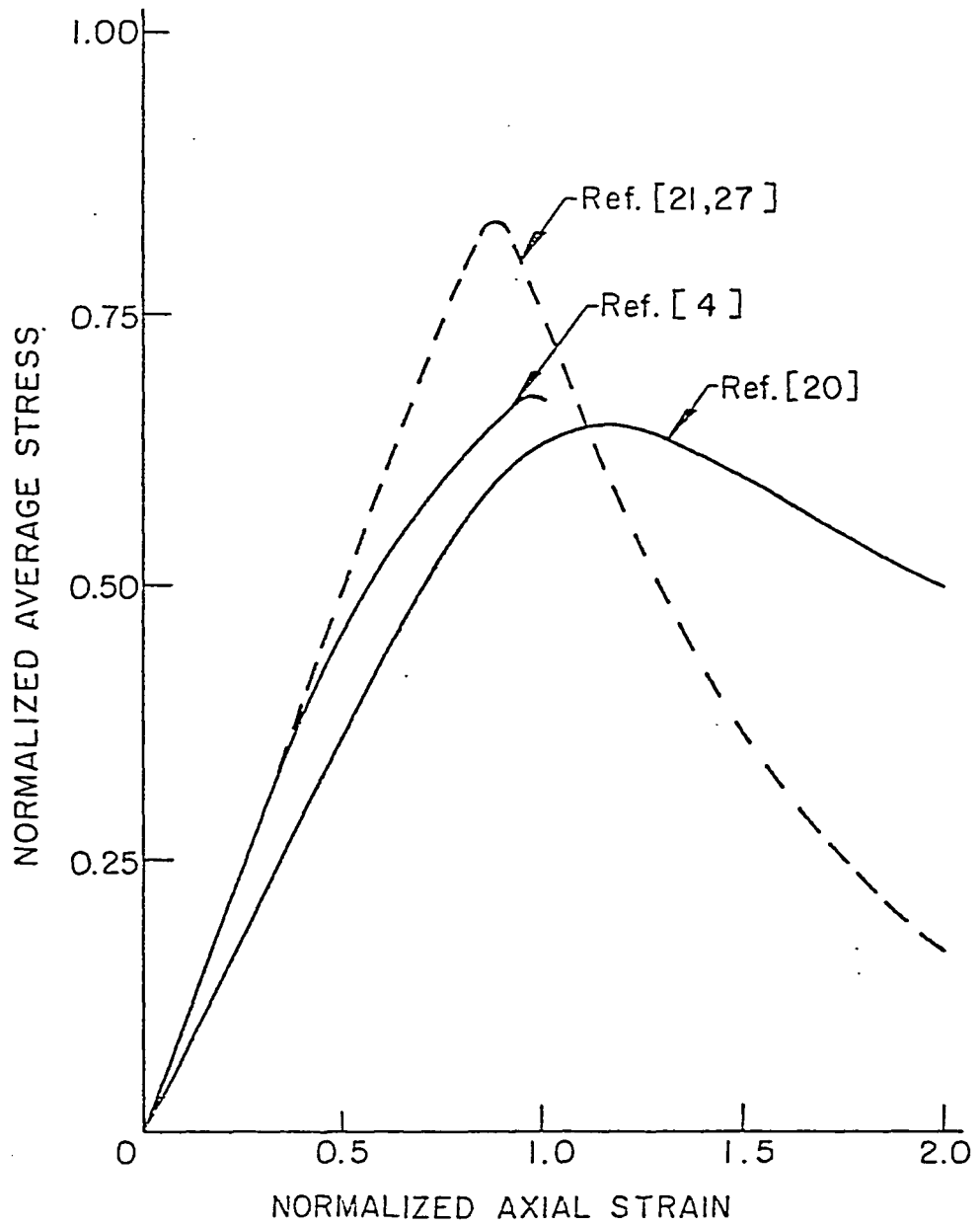
Fig.5 Load Response of Compression Flange for Lehigh Specimen
by Three Methods
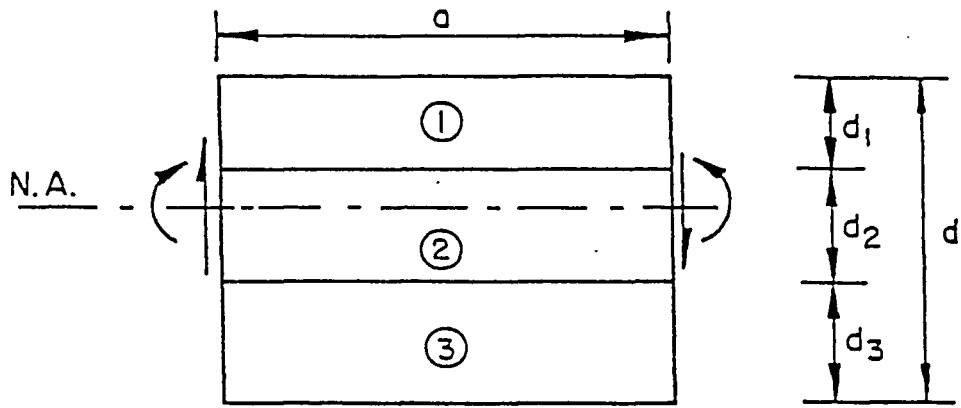
Segment of Web   (i) : Subpanel No.
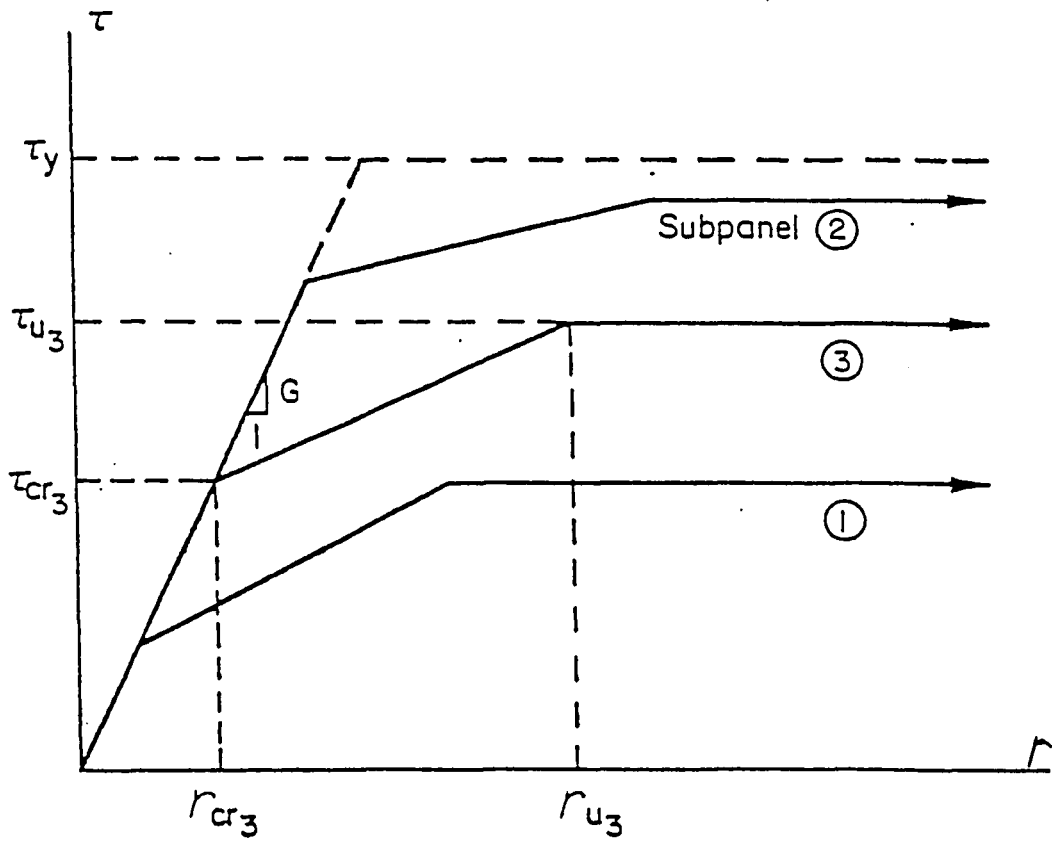
Fig.6   Shear Behavior of Web Subpanels
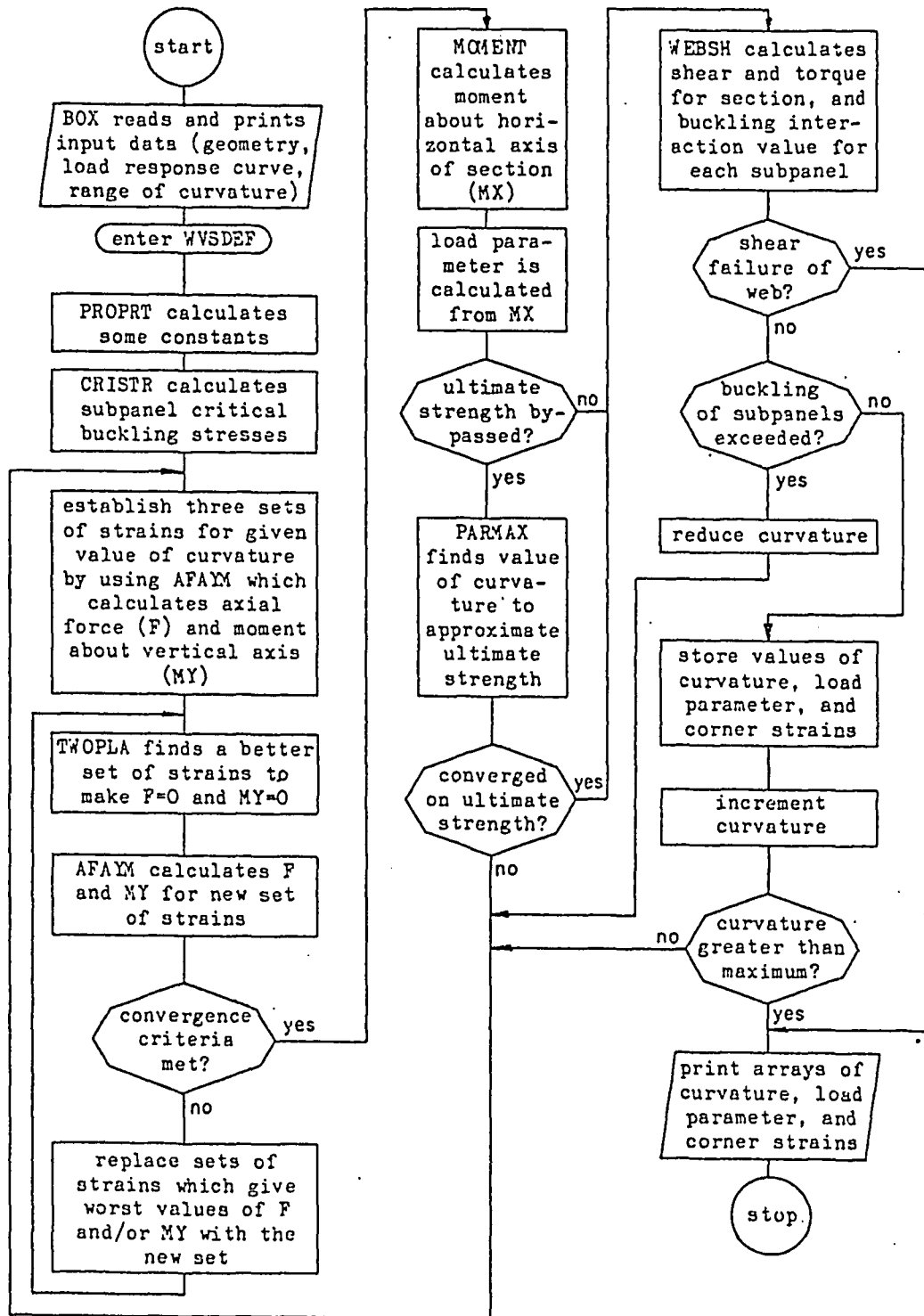
Fig.7 General Flowchart

62
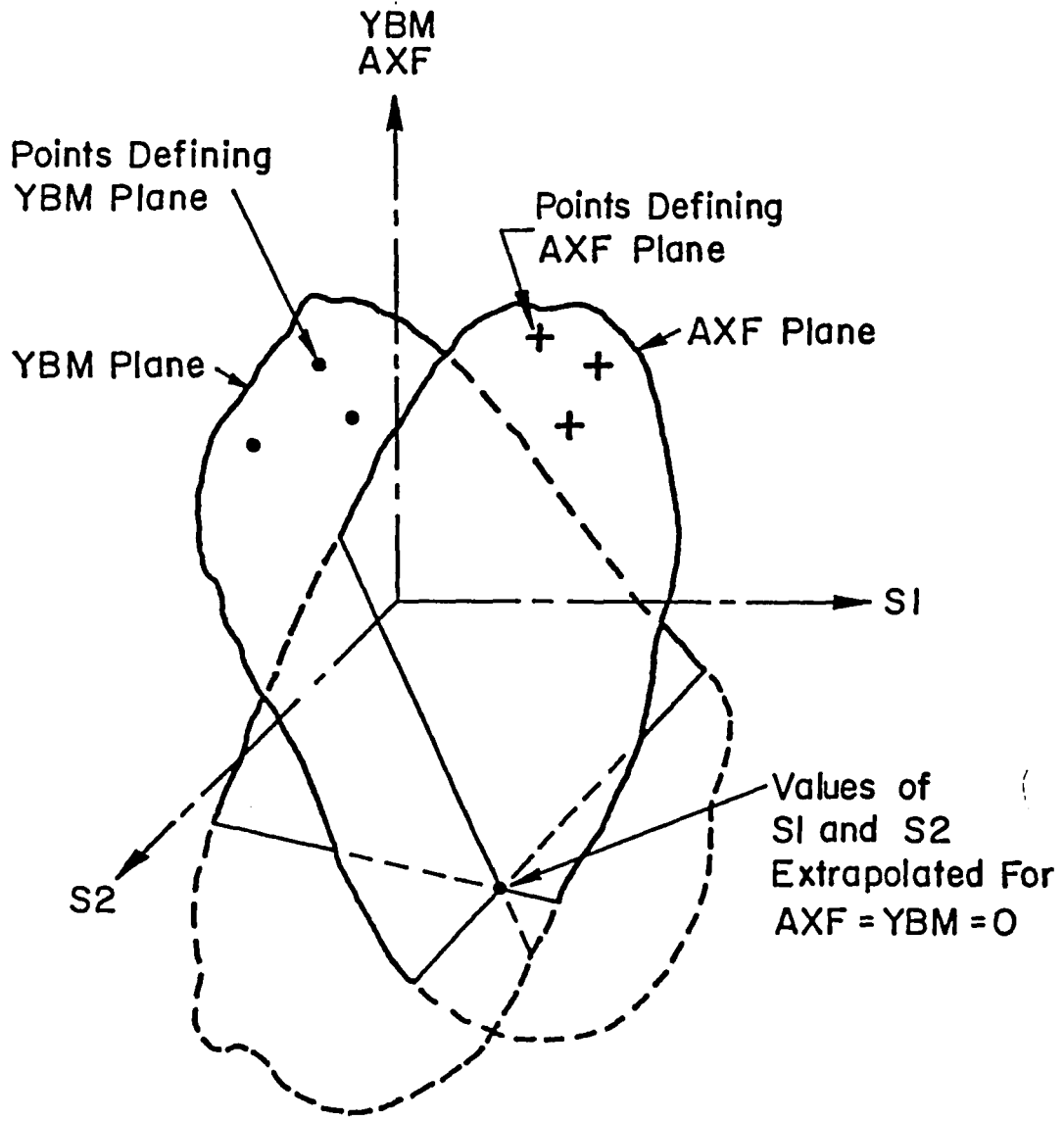
Fig.8 Use of Tangent Planes for Equilibrium Convergence

Compressive Strains (–)
Tensile Strains (+)
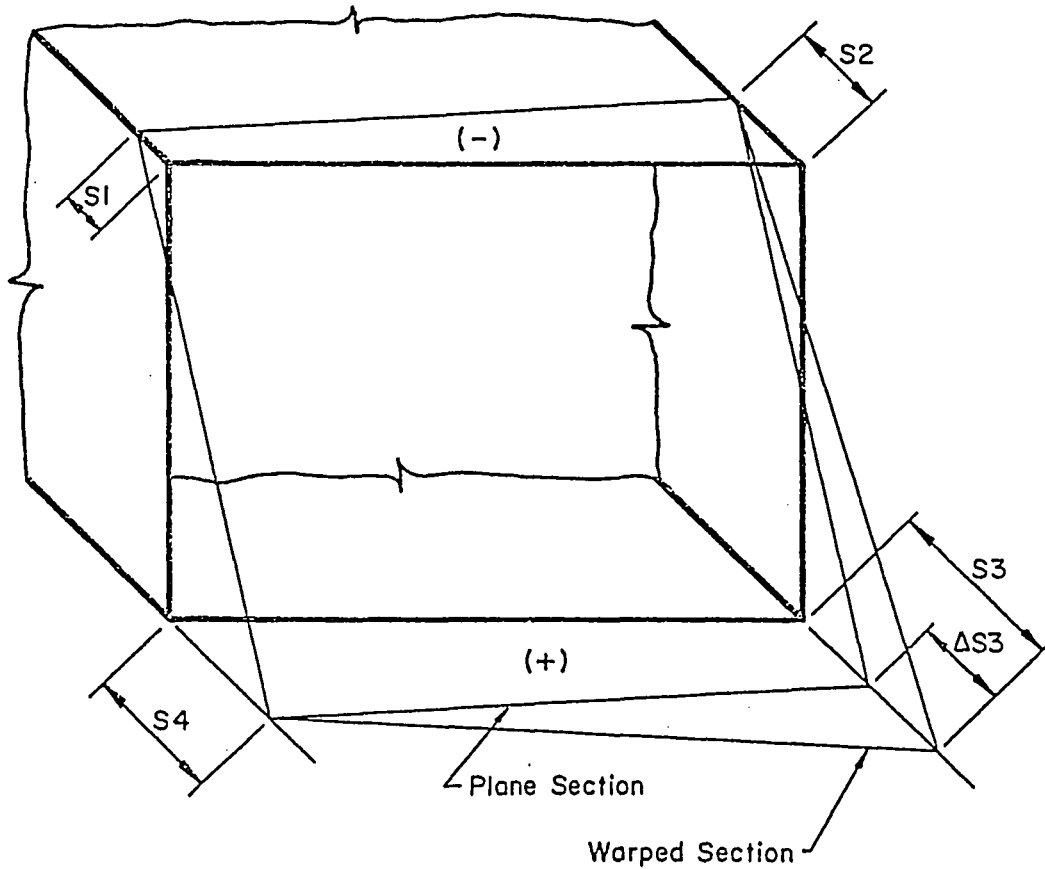
Degree of Warping

$$SWP = \frac{\Delta S3}{2(S4 - S1)}$$

Fig.9   Strain Distribution and Definition of Warping
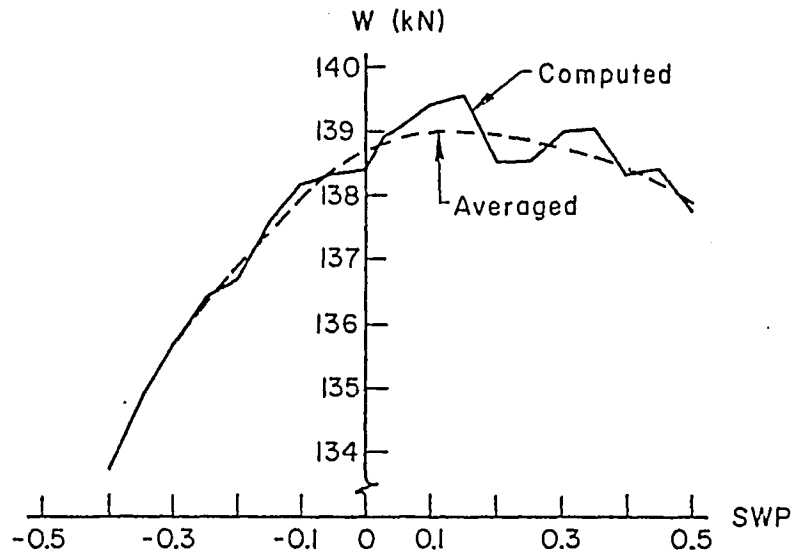
(a) W vs. SWP
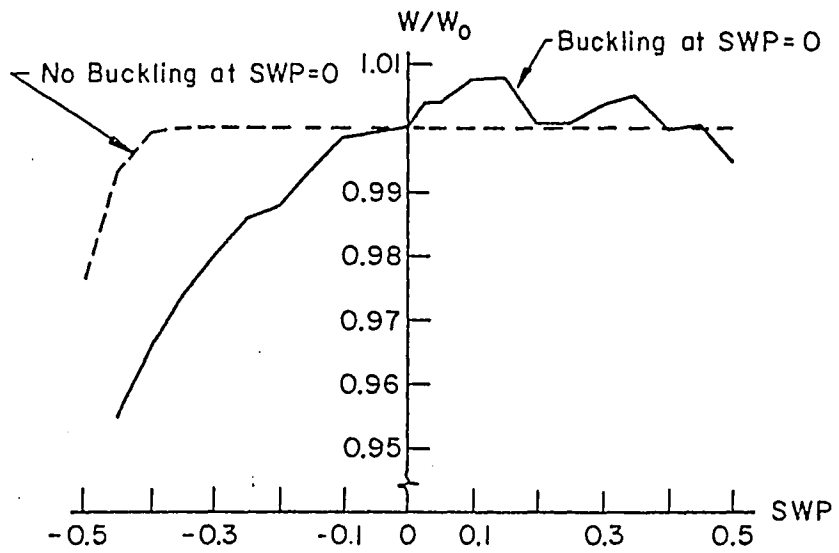
(b) Effect of web buckling on W vs. SWP

Fig.10   Load Parameter vs. Degree of Warping

Test Segment

W

M = 0.562W(kN-m)
V = 0.615W(kN)
T = 0 (kN-m)

508

3 @ 457

1829   1143

2972

a) Test 1 : Moment + Shear

W

M = 0.616W(kN-m)
V = 0.385W(kN)
T = 0.194W(kN-m)
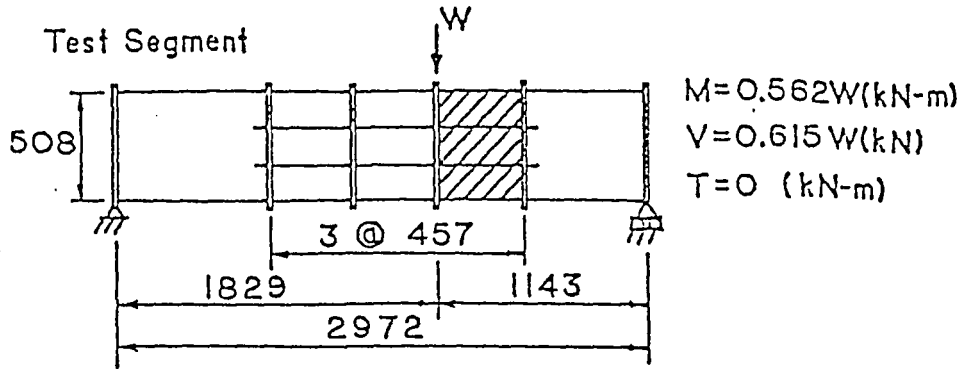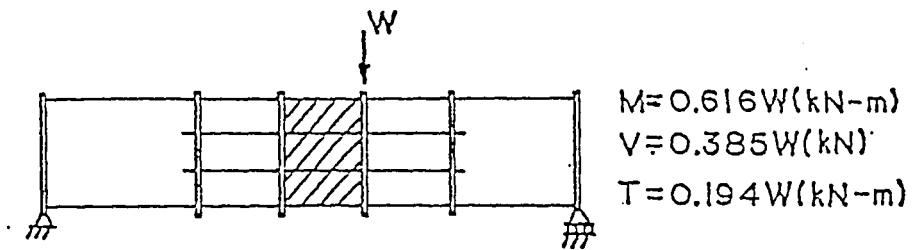
b) Test 2 : Moment + Shear + Torque

W

M = 0.615W(kN-m)
V = 0.538W(kN)
T = 0.200W(kN-m)
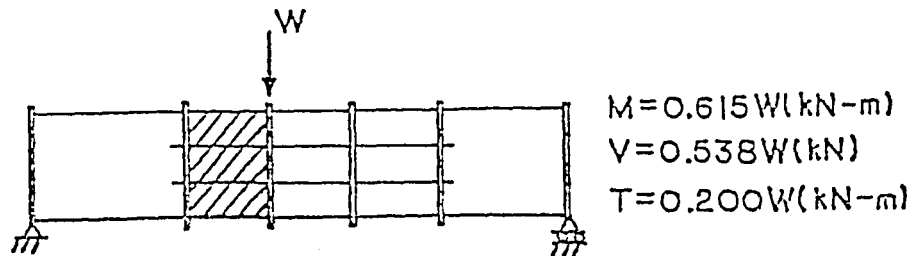
b) Test 3 : Moment + Shear + Torque

Fig.11   General View of the Lehigh Test Specimen
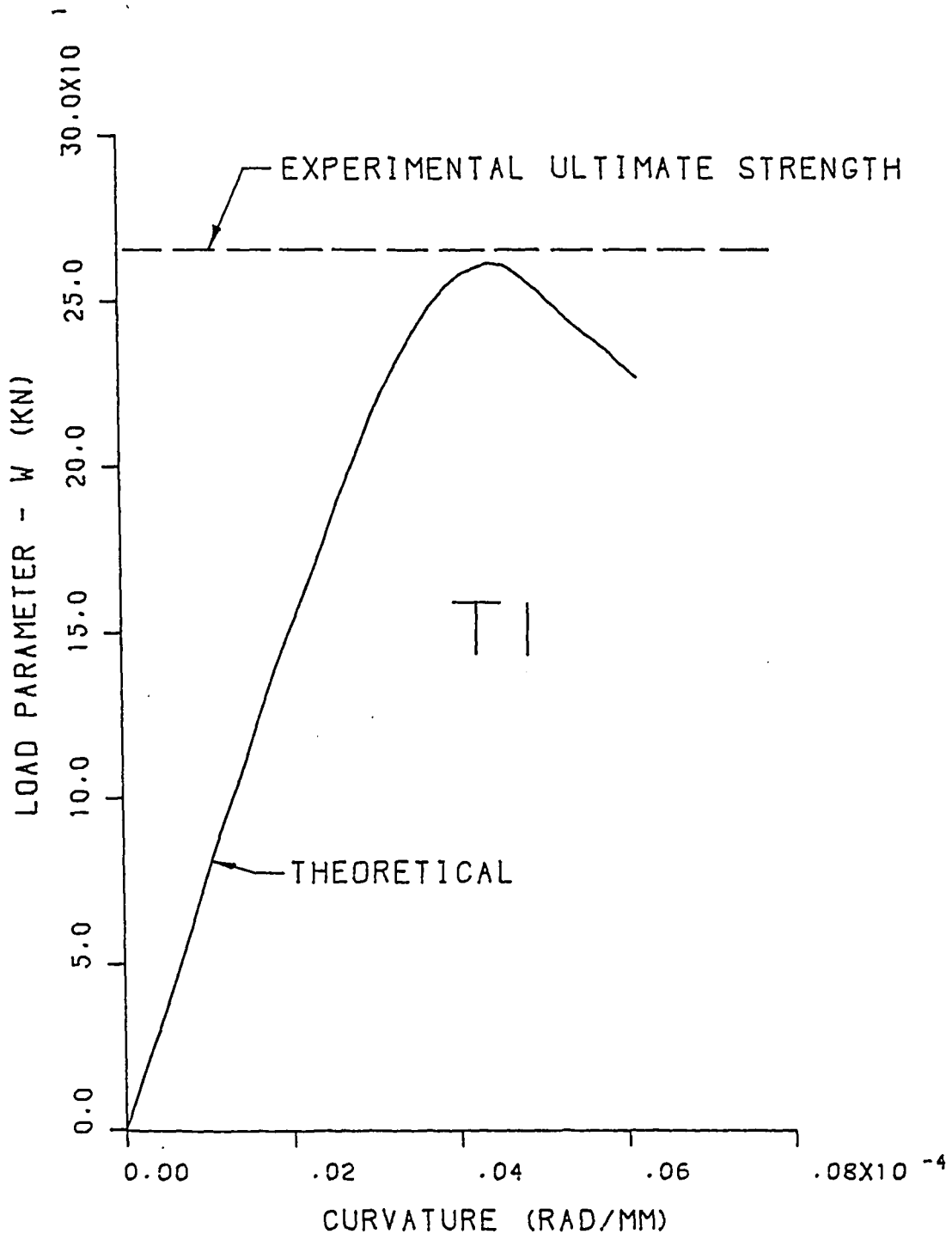
Fig.12 Lehigh – Test 1
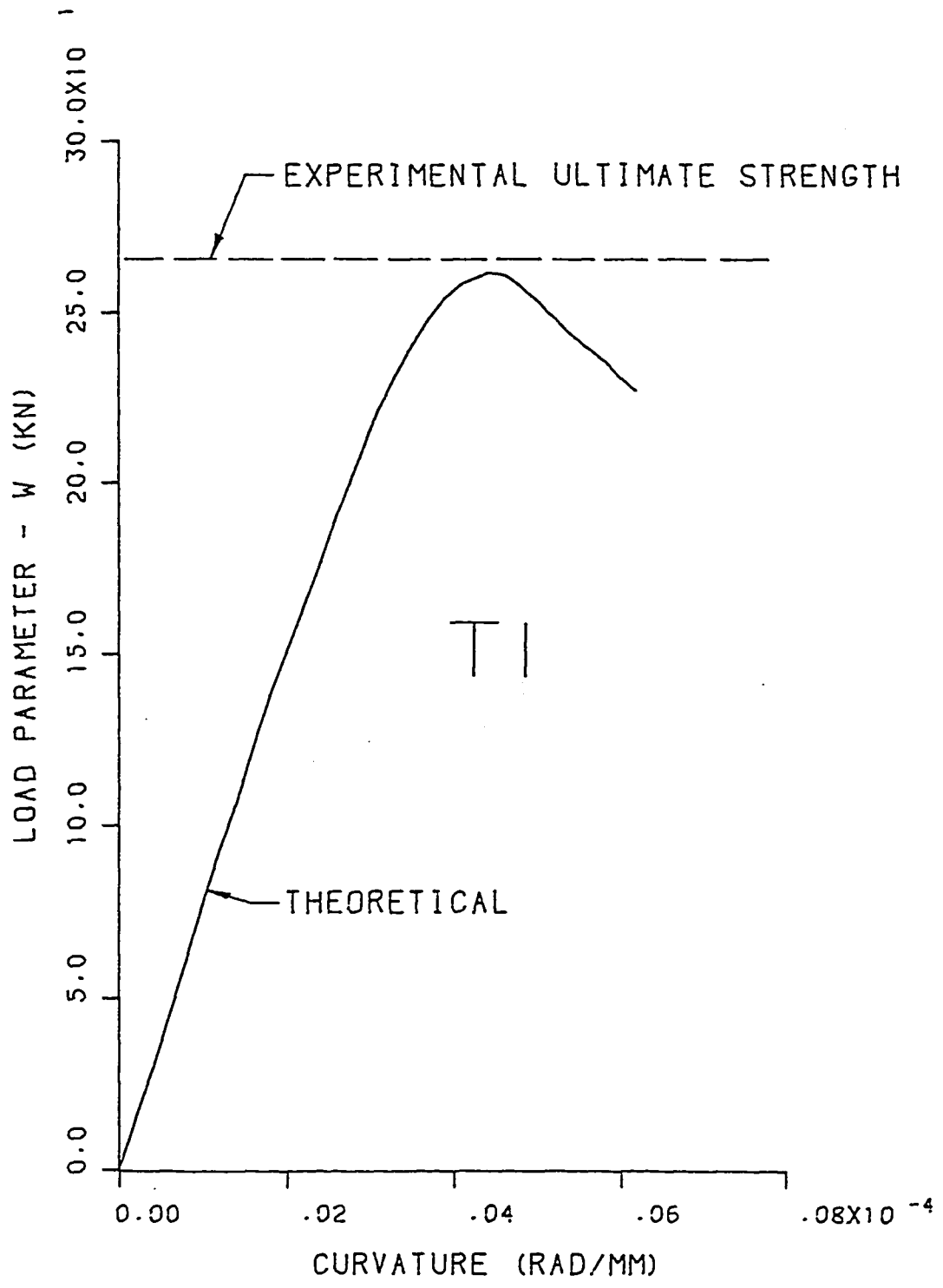
Fig.12 Lehigh – Test 1
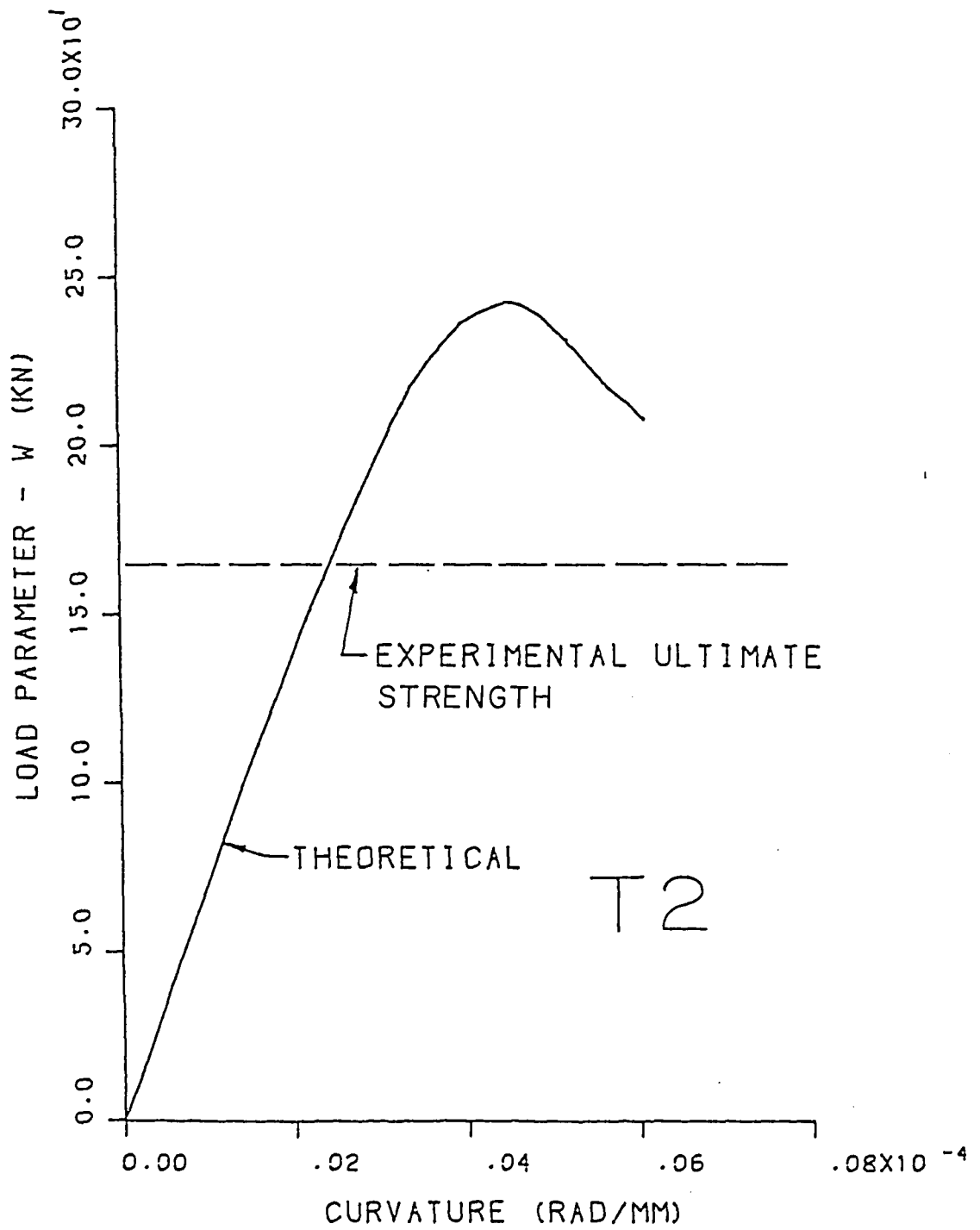
Fig.13 Lehigh — Test 2
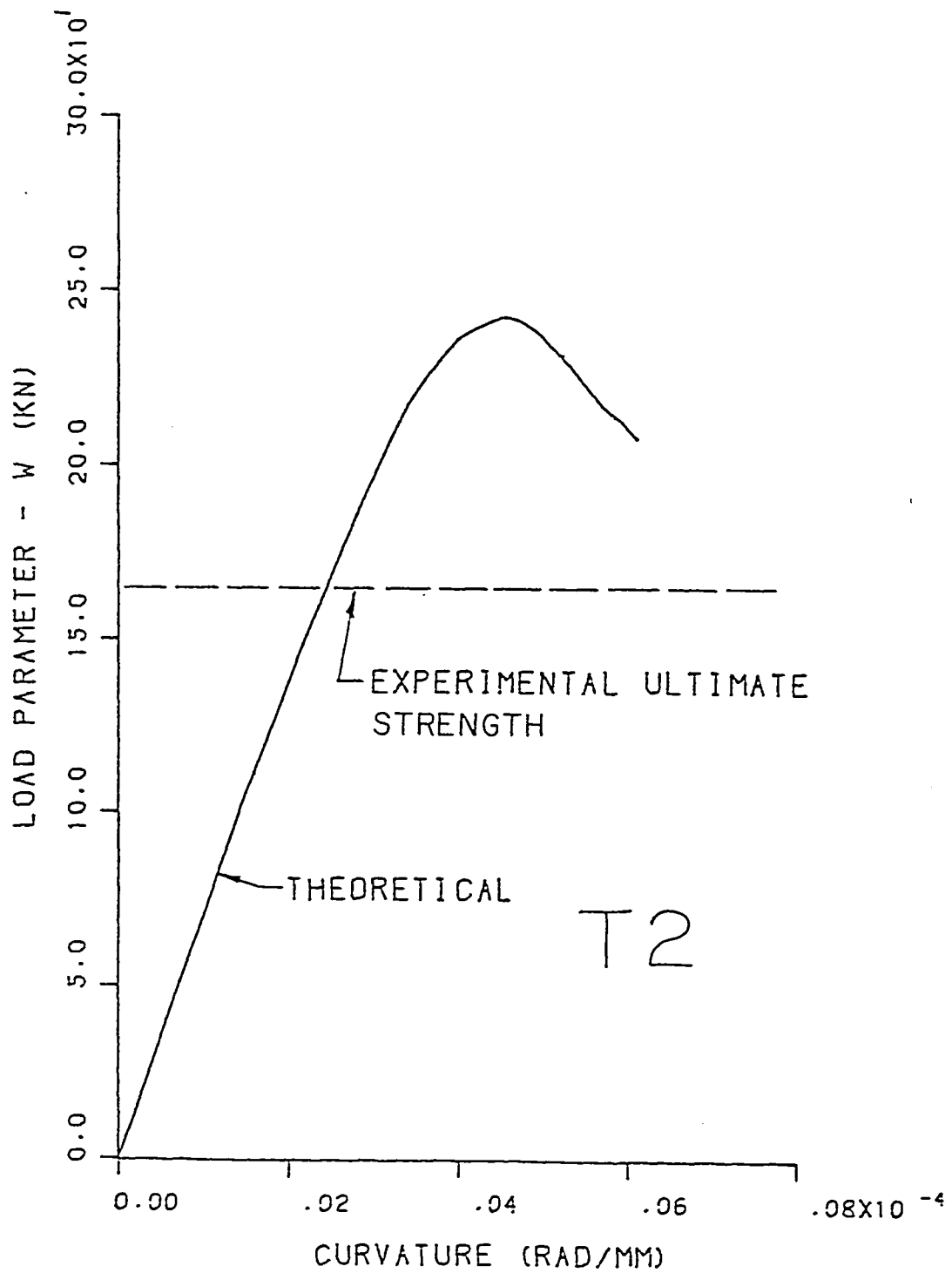
Fig.13 Lehigh — Test 2
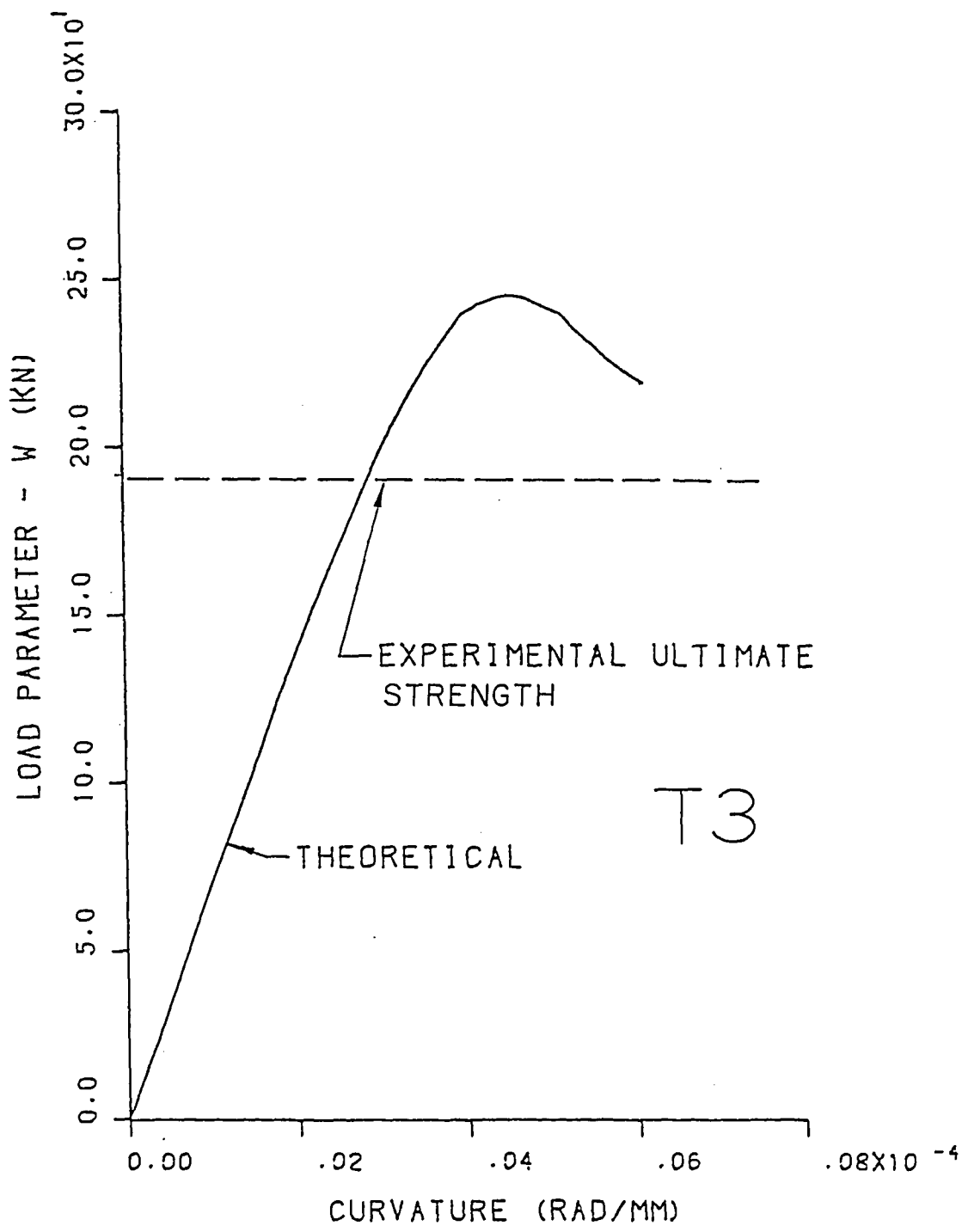
Fig.14 Lehigh – Test 3
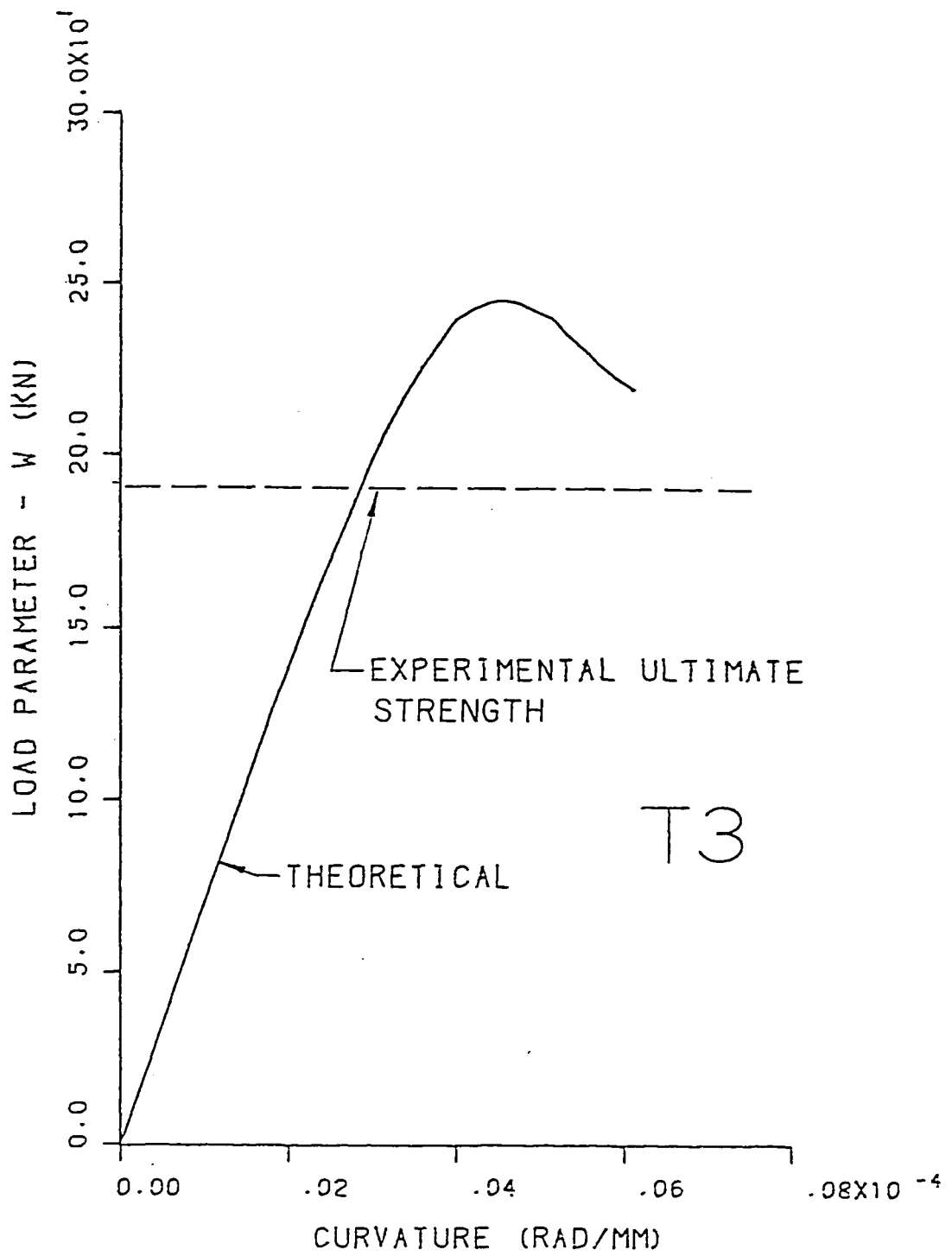
Fig.14 Lehigh – Test 3
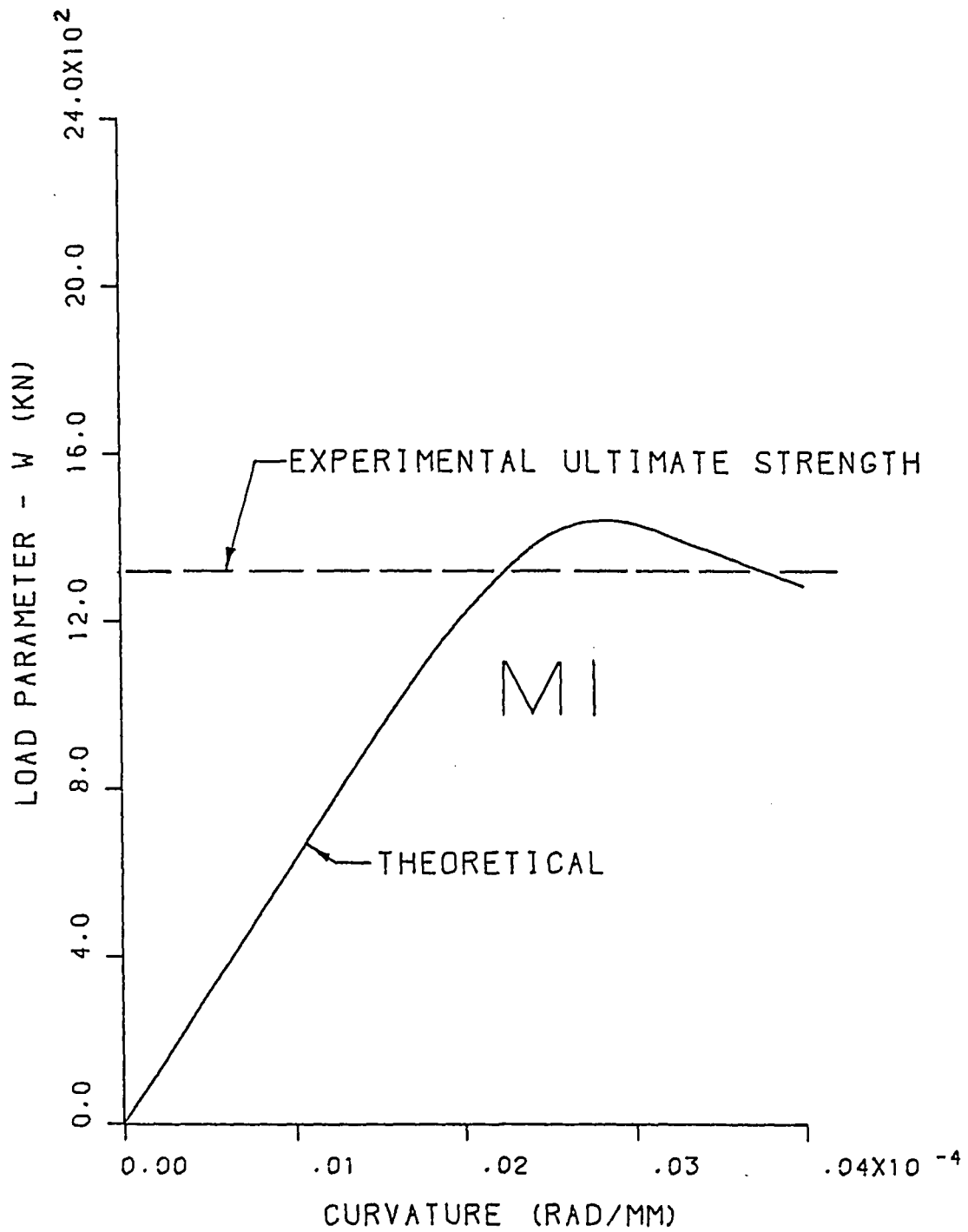
Fig.15   Imperial College – Model 1
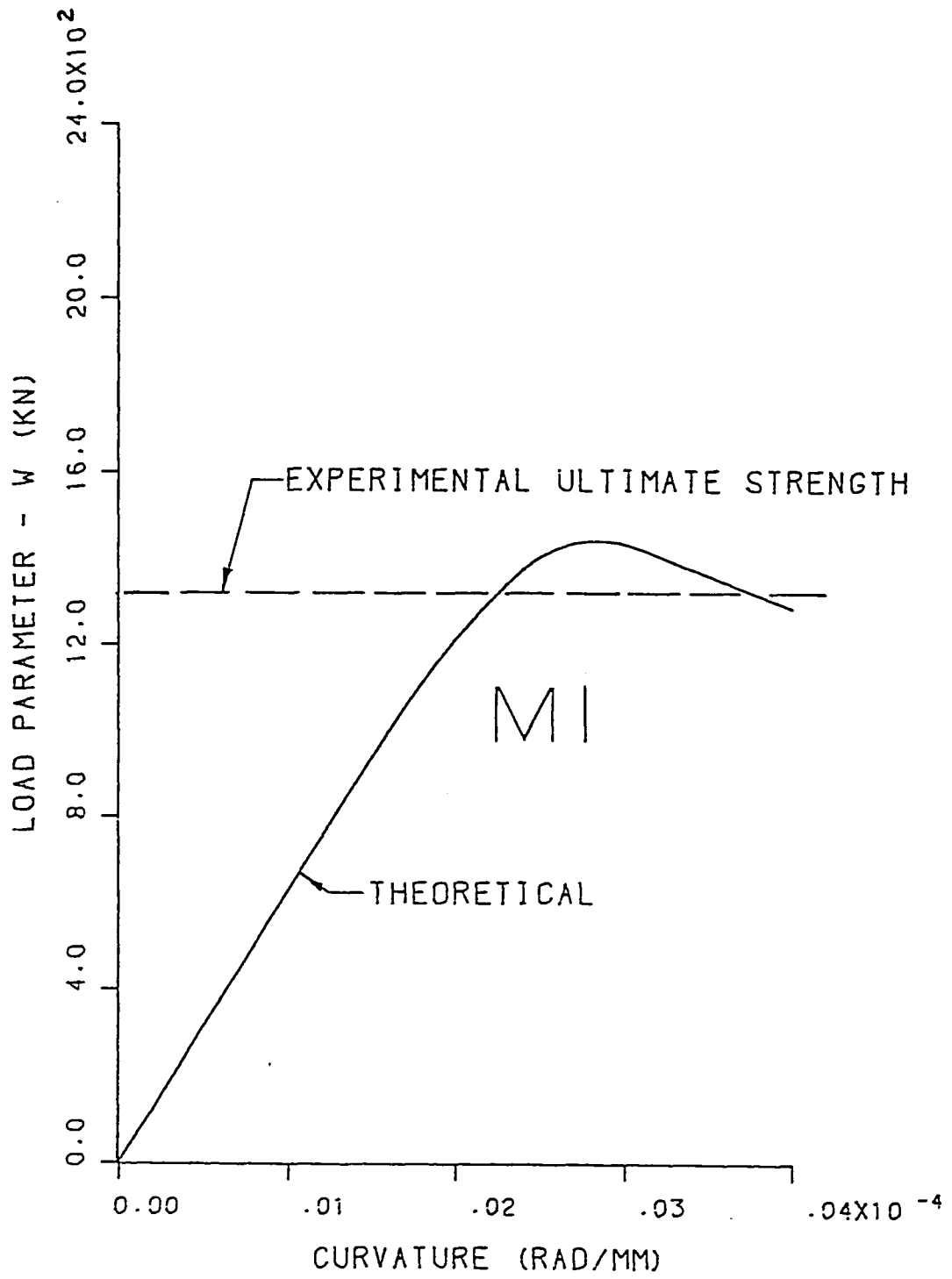
Fig.15 Imperial College – Model 1

Fig.16 Imperial College - Model 2

71
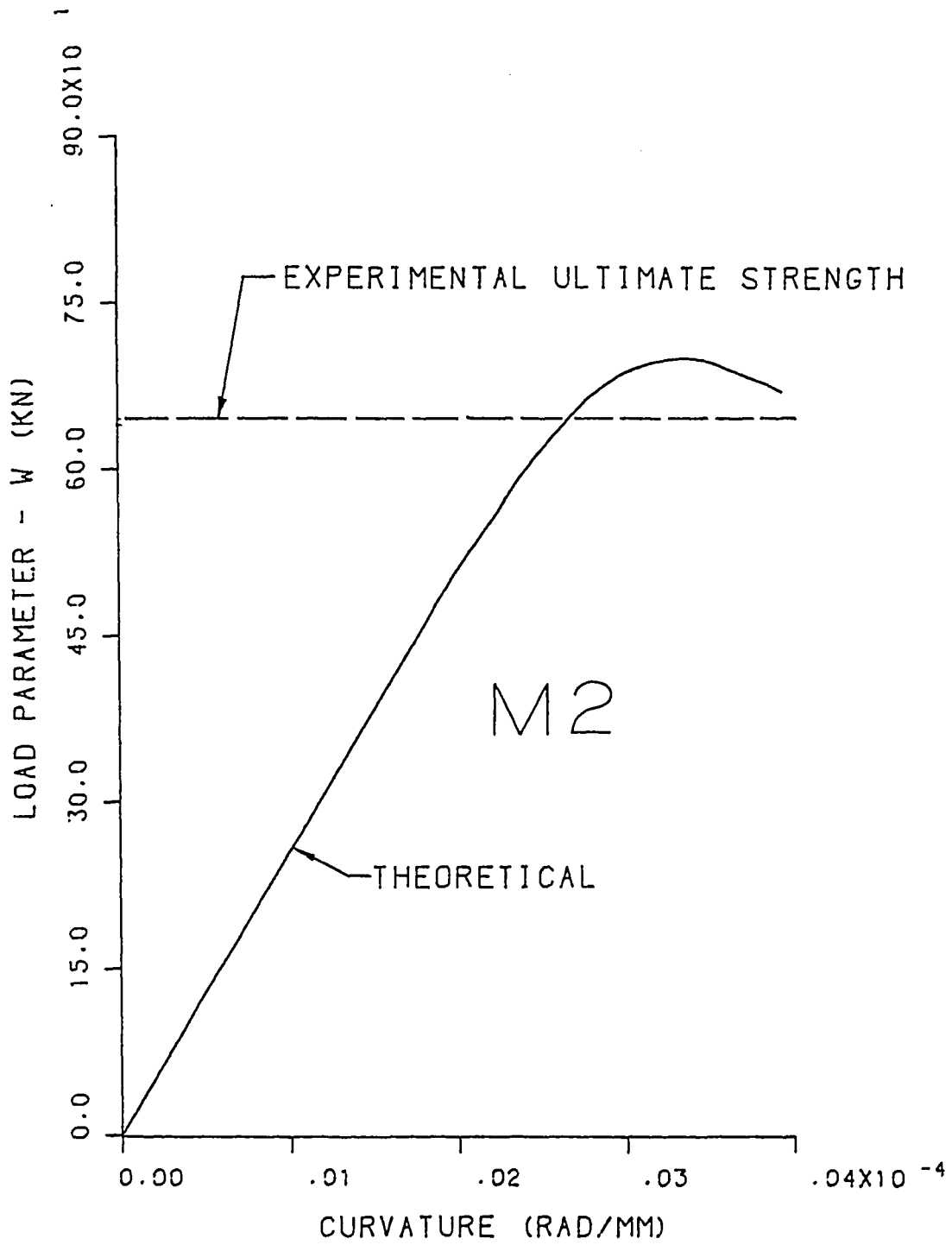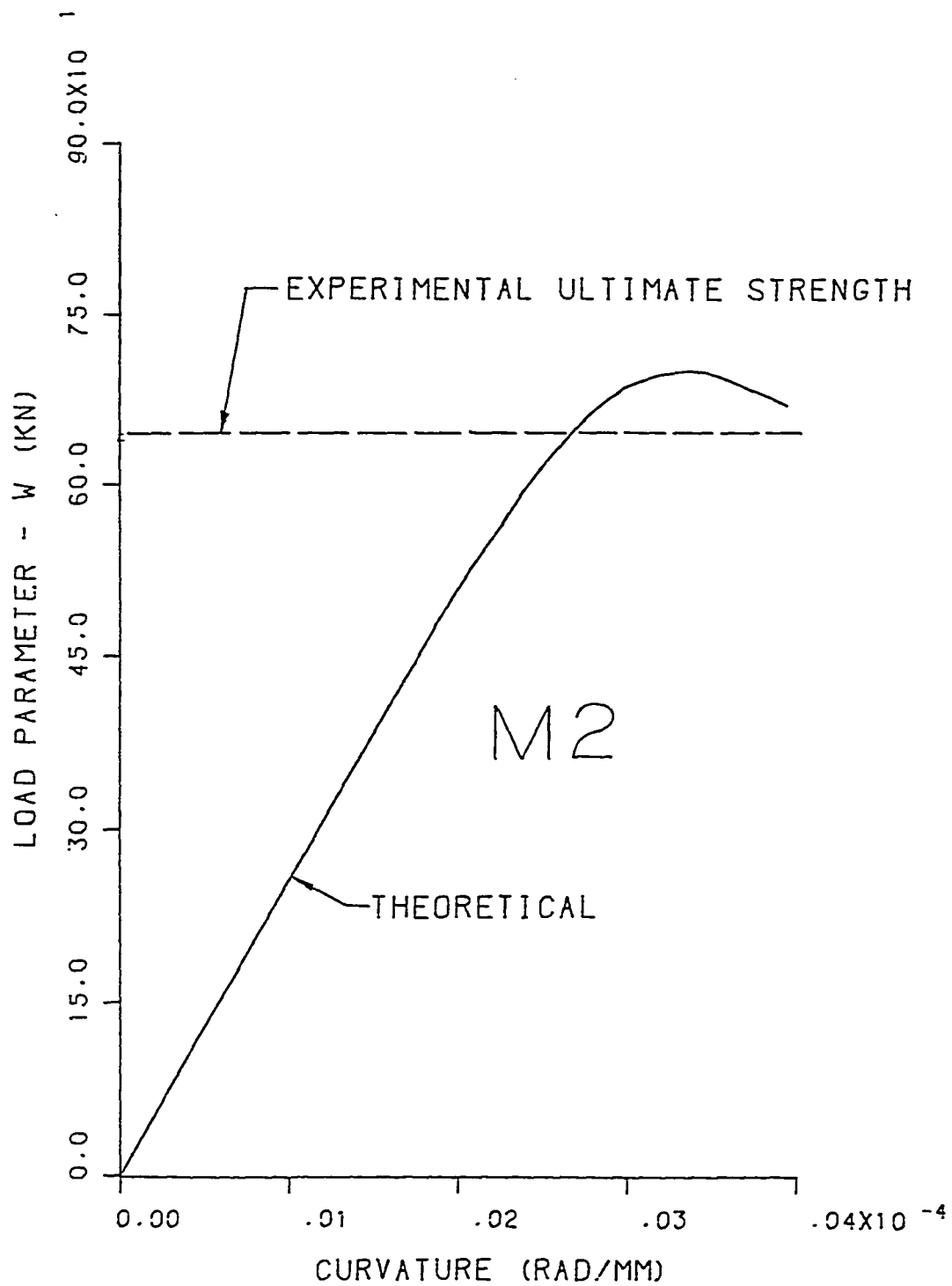
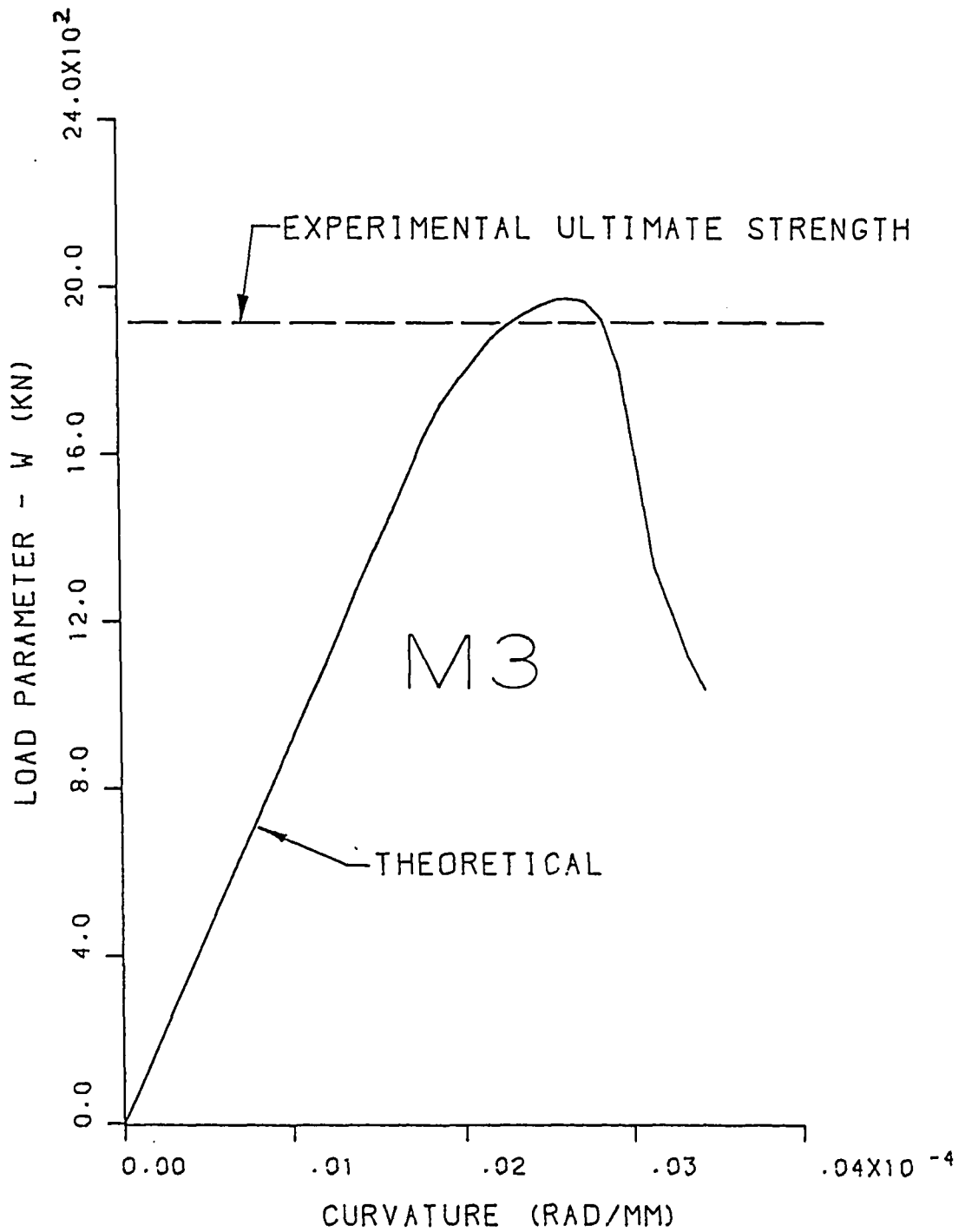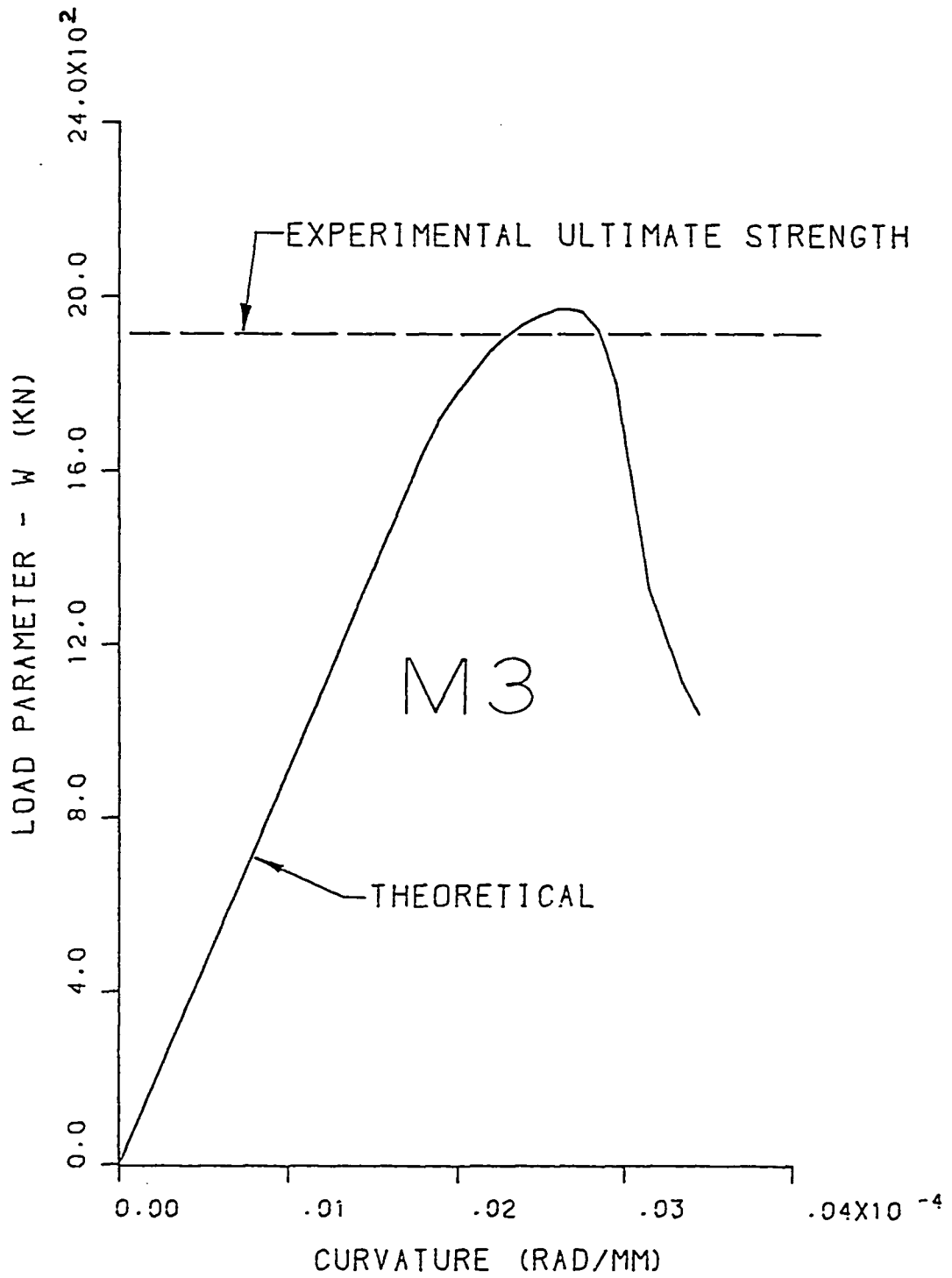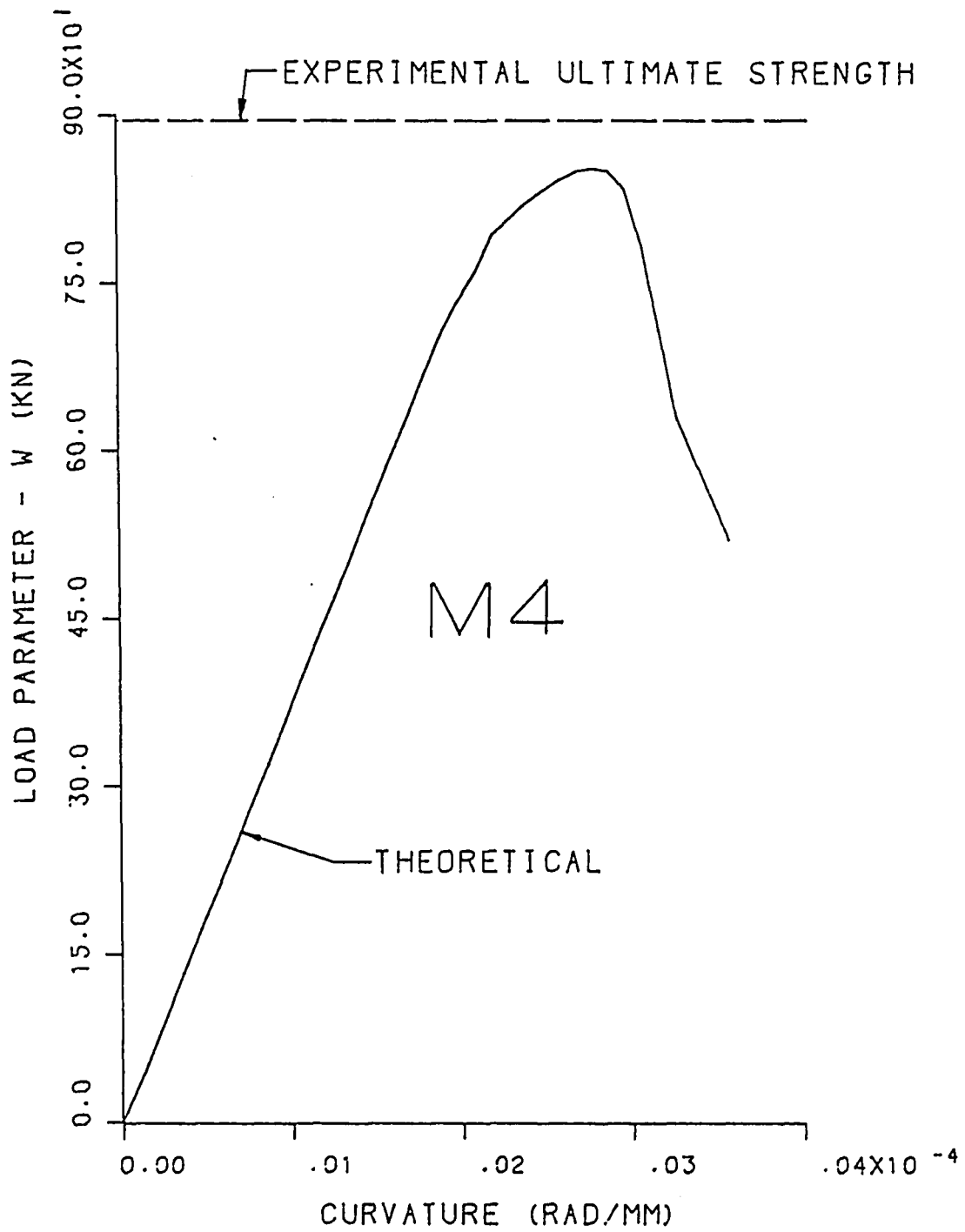Fig.16   Imperial College – Model 2

Fig.17 Imperial College – Model 3

Fig.17 Imperial College – Model 3

72
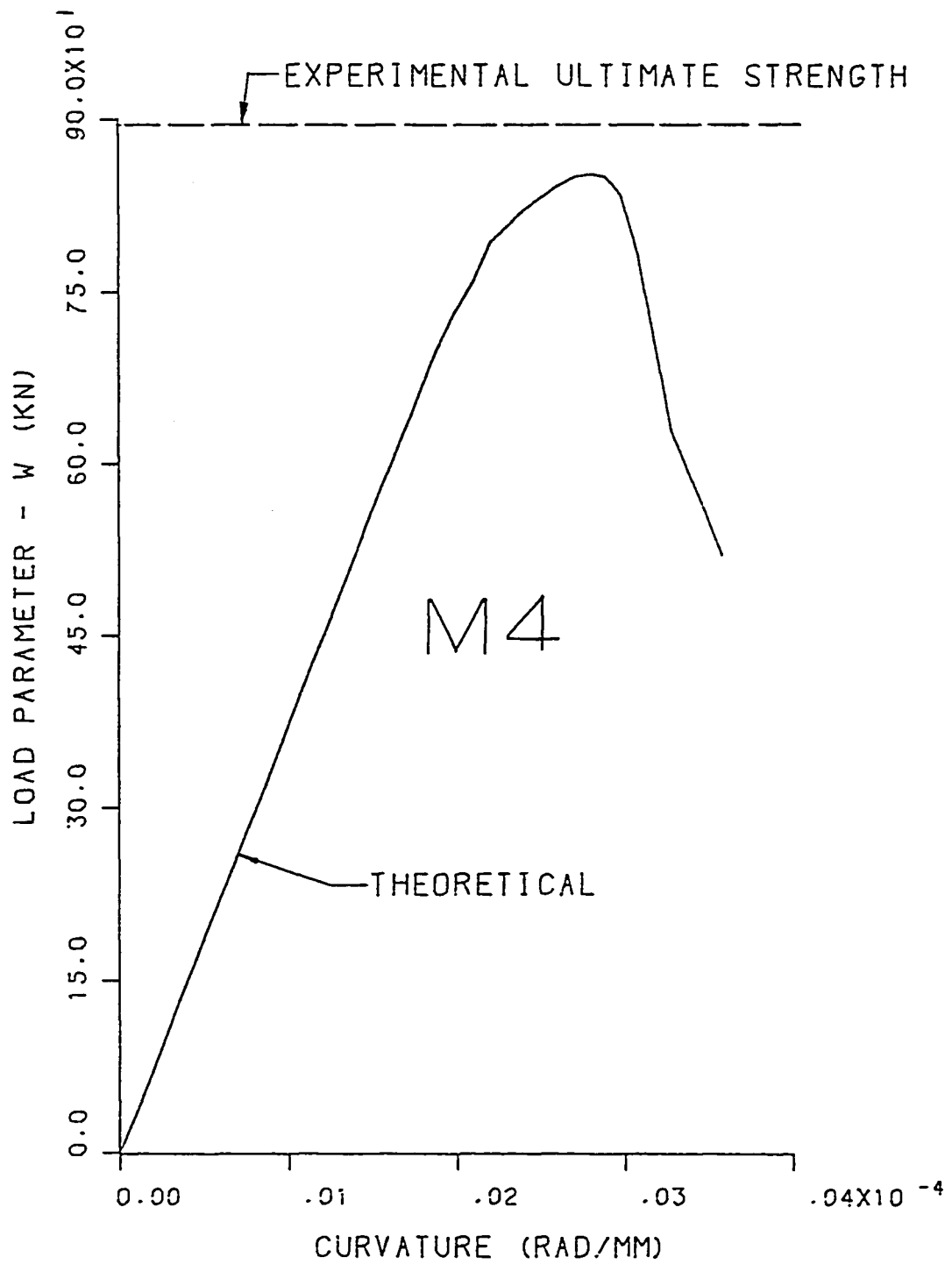
Fig.18 Imperial College – Model 4

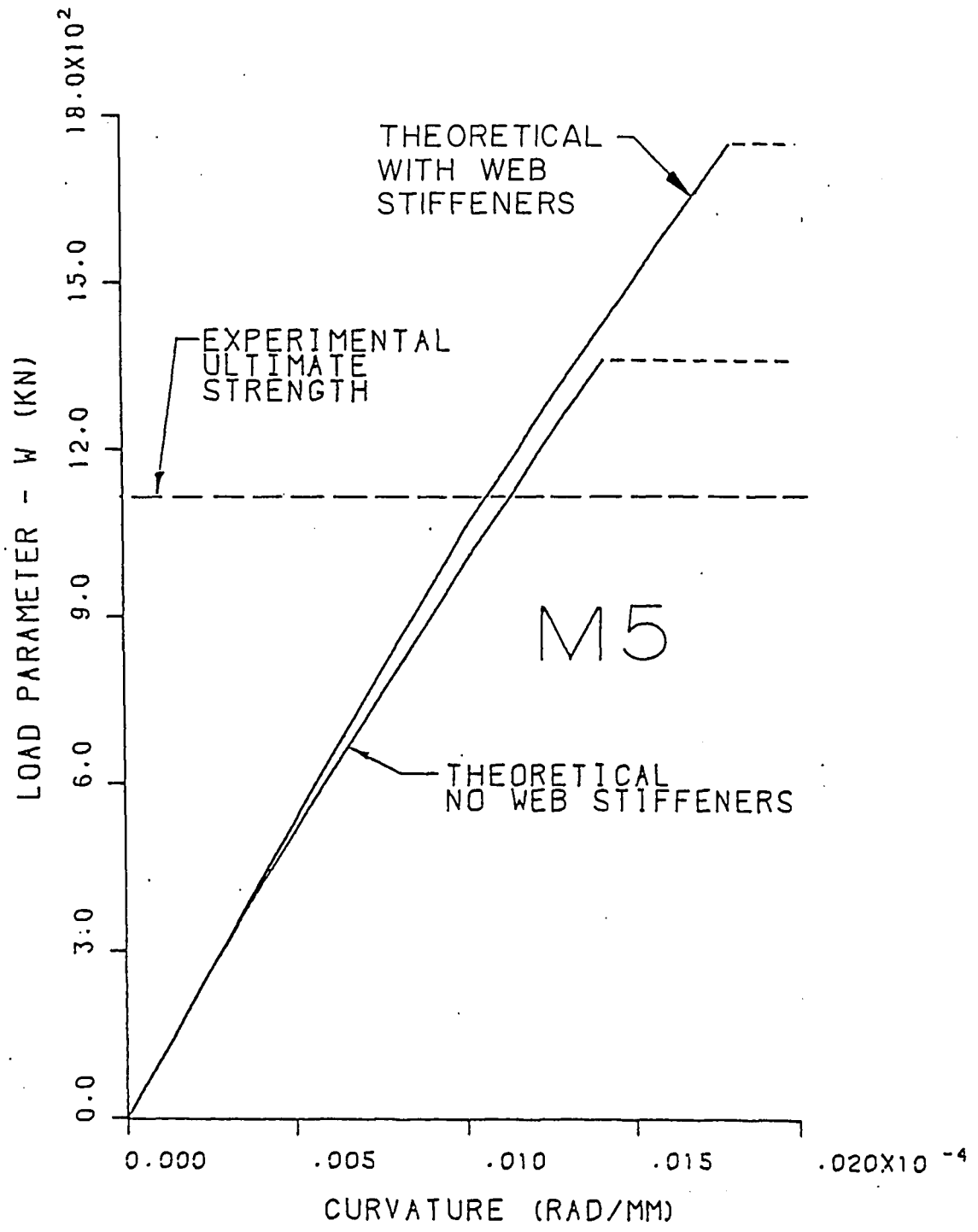73

Fig.18　Imperial College — Model 4
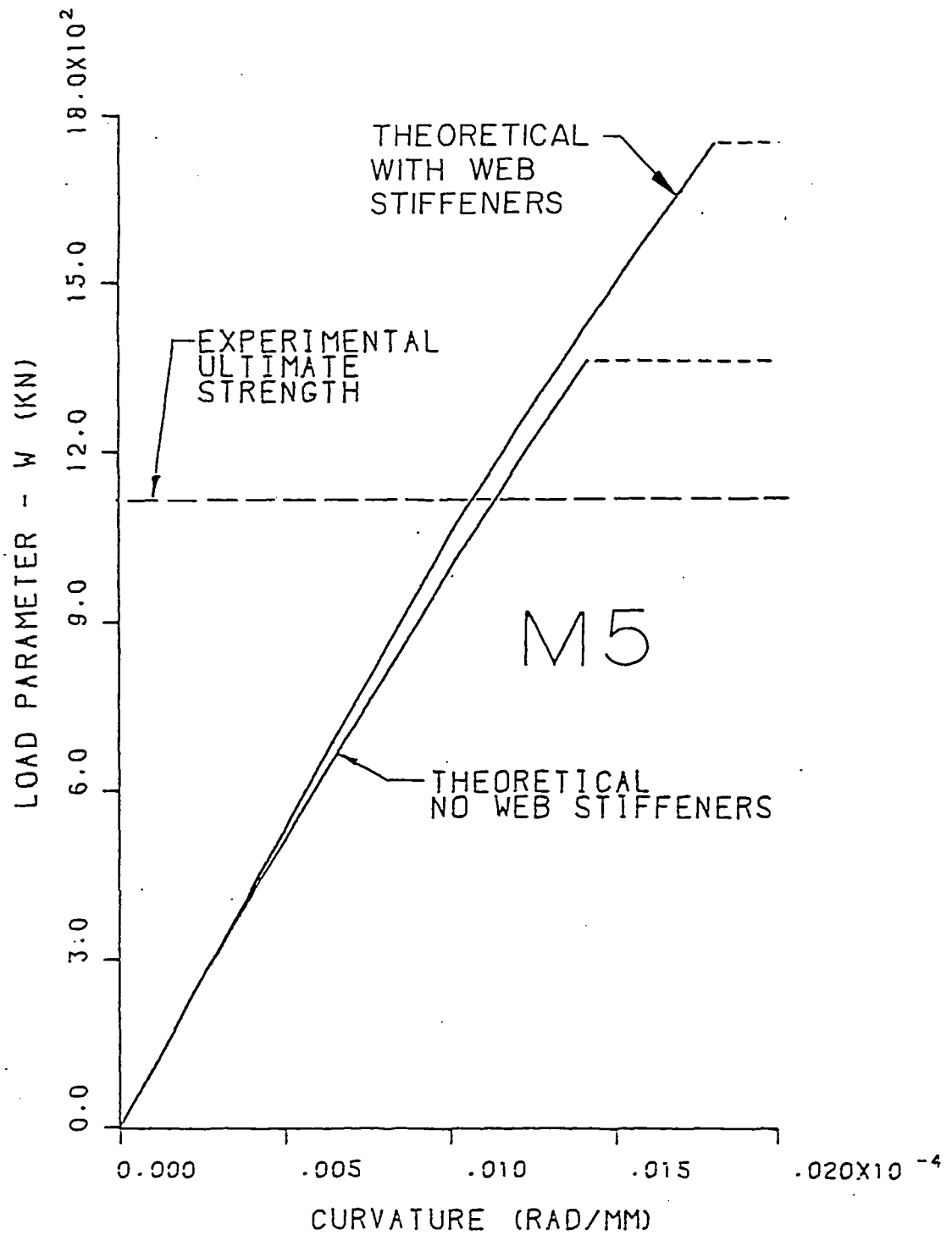
Fig.19   Imperial College – Model 5
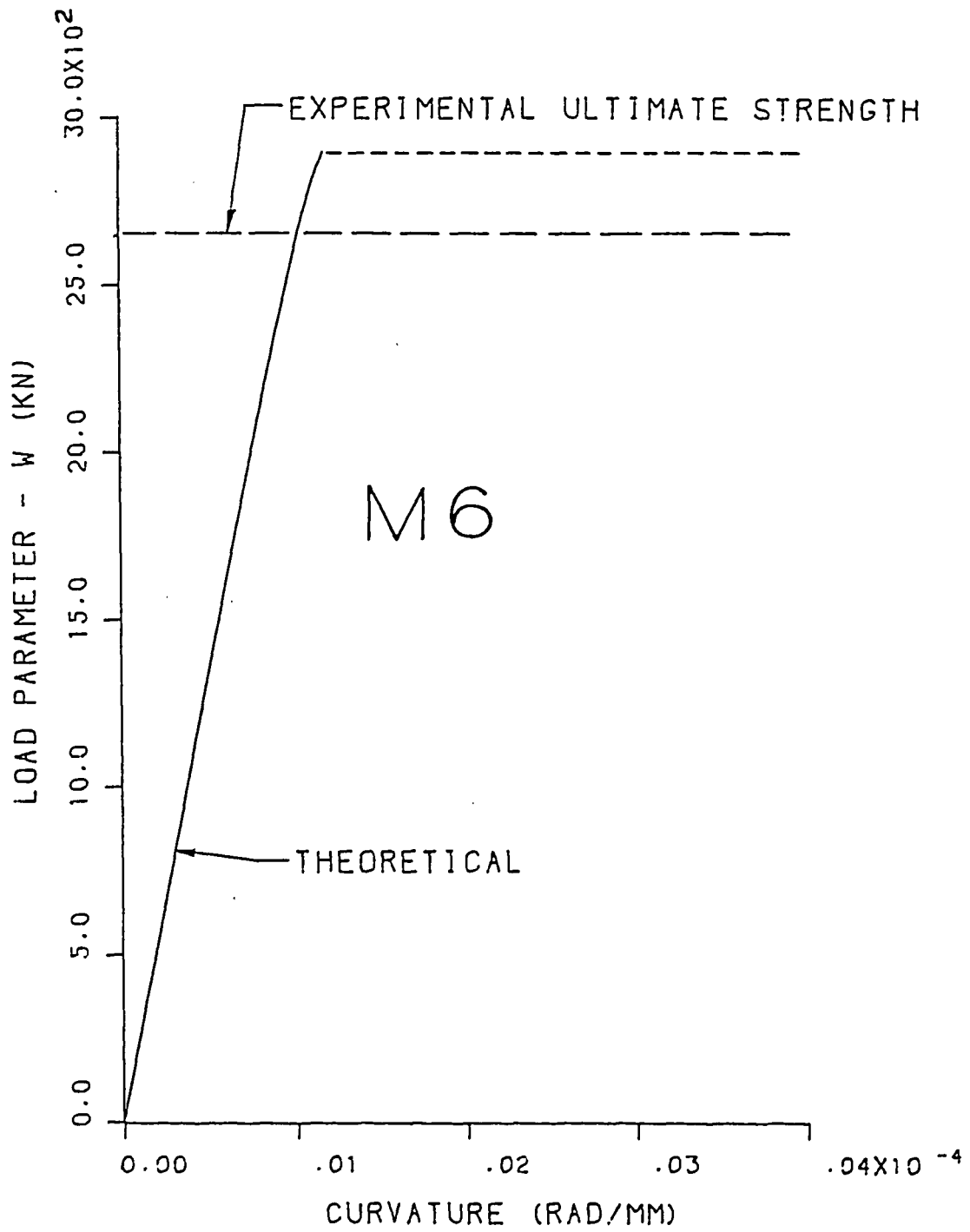
74

Fig.19 Imperial College – Model 5

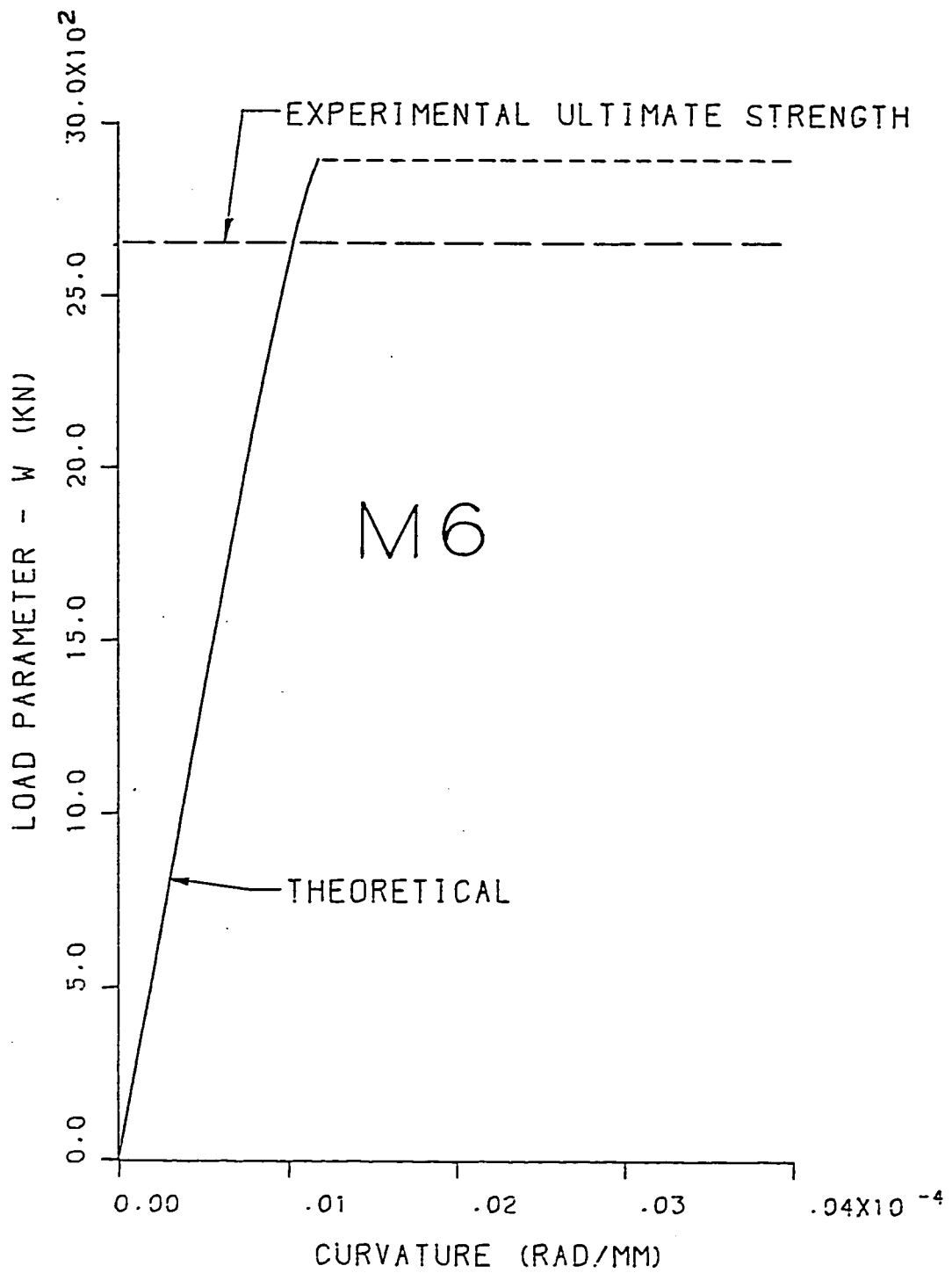Fig.20   Imperial College — Model 6

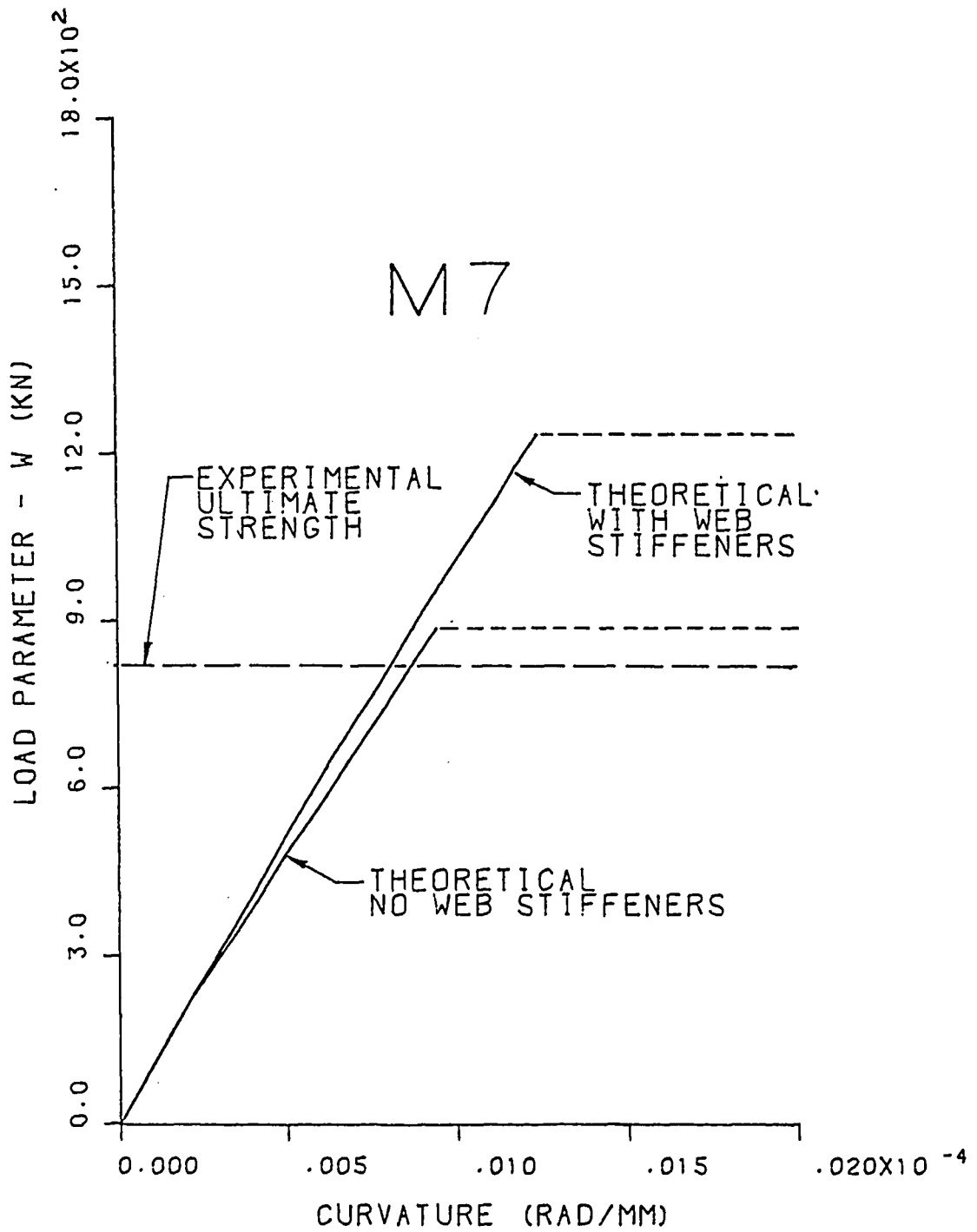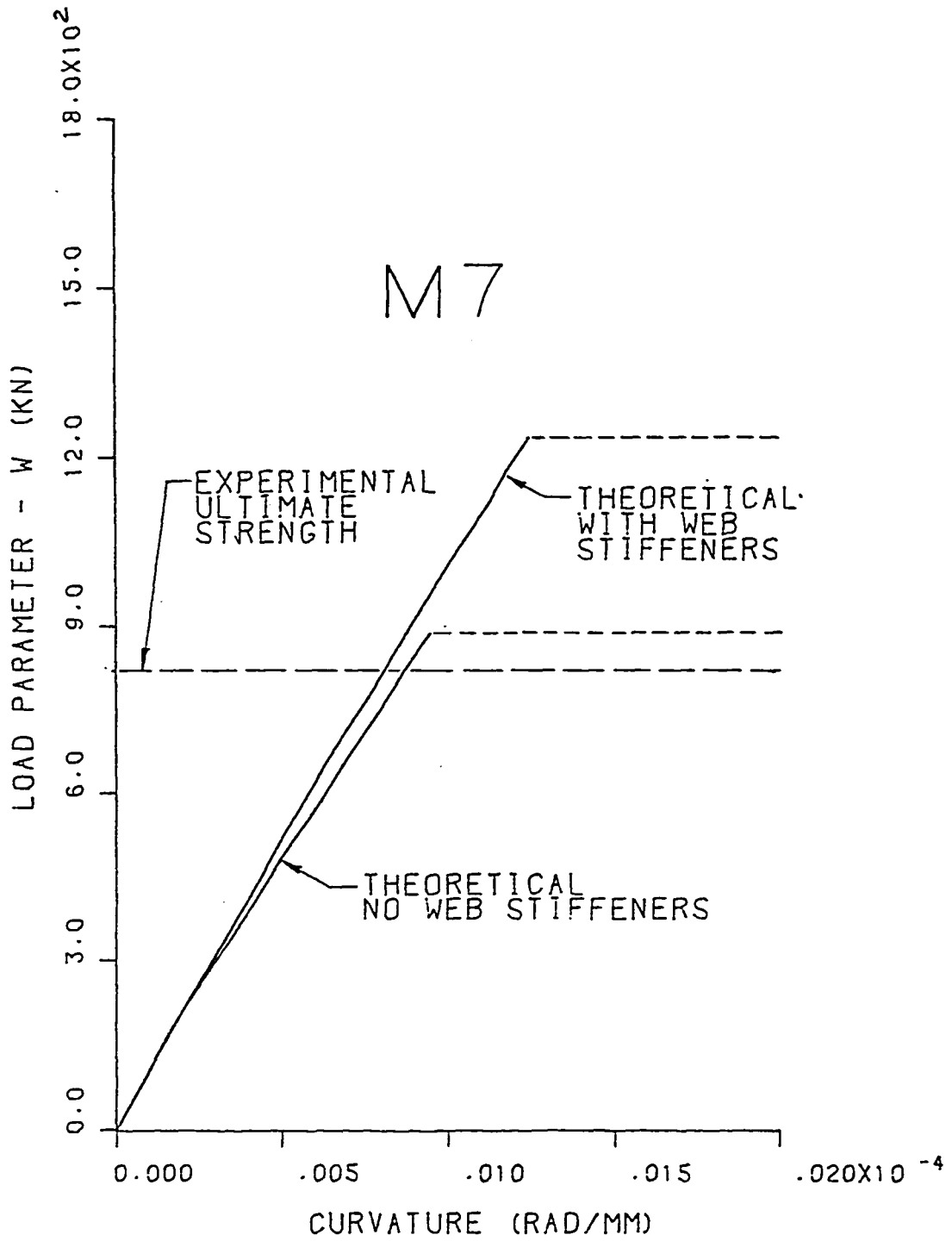Fig.20 Imperial College – Model 6

Fig.21   Imperial College – Model 7
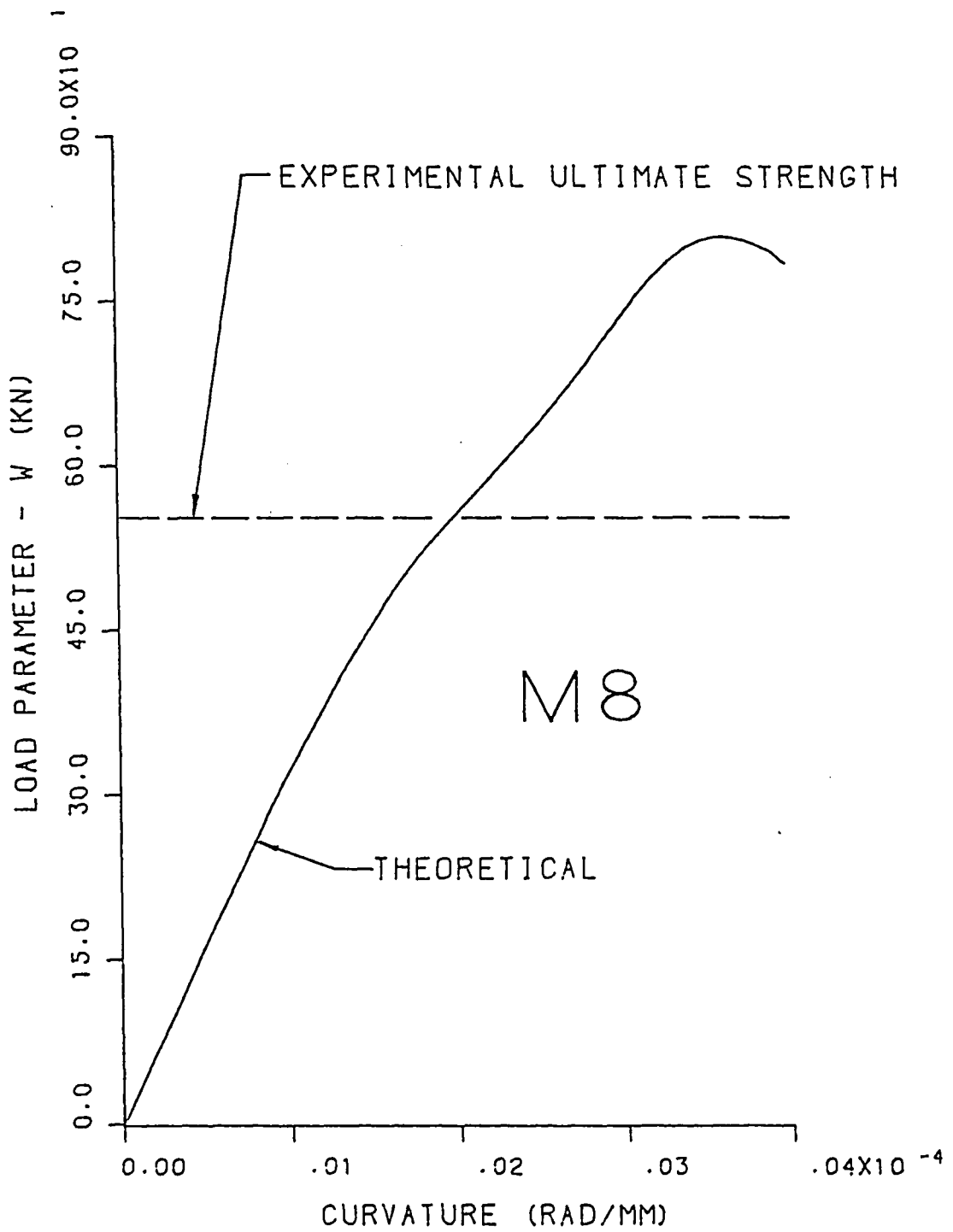
Fig.21 Imperial College – Model 7

76

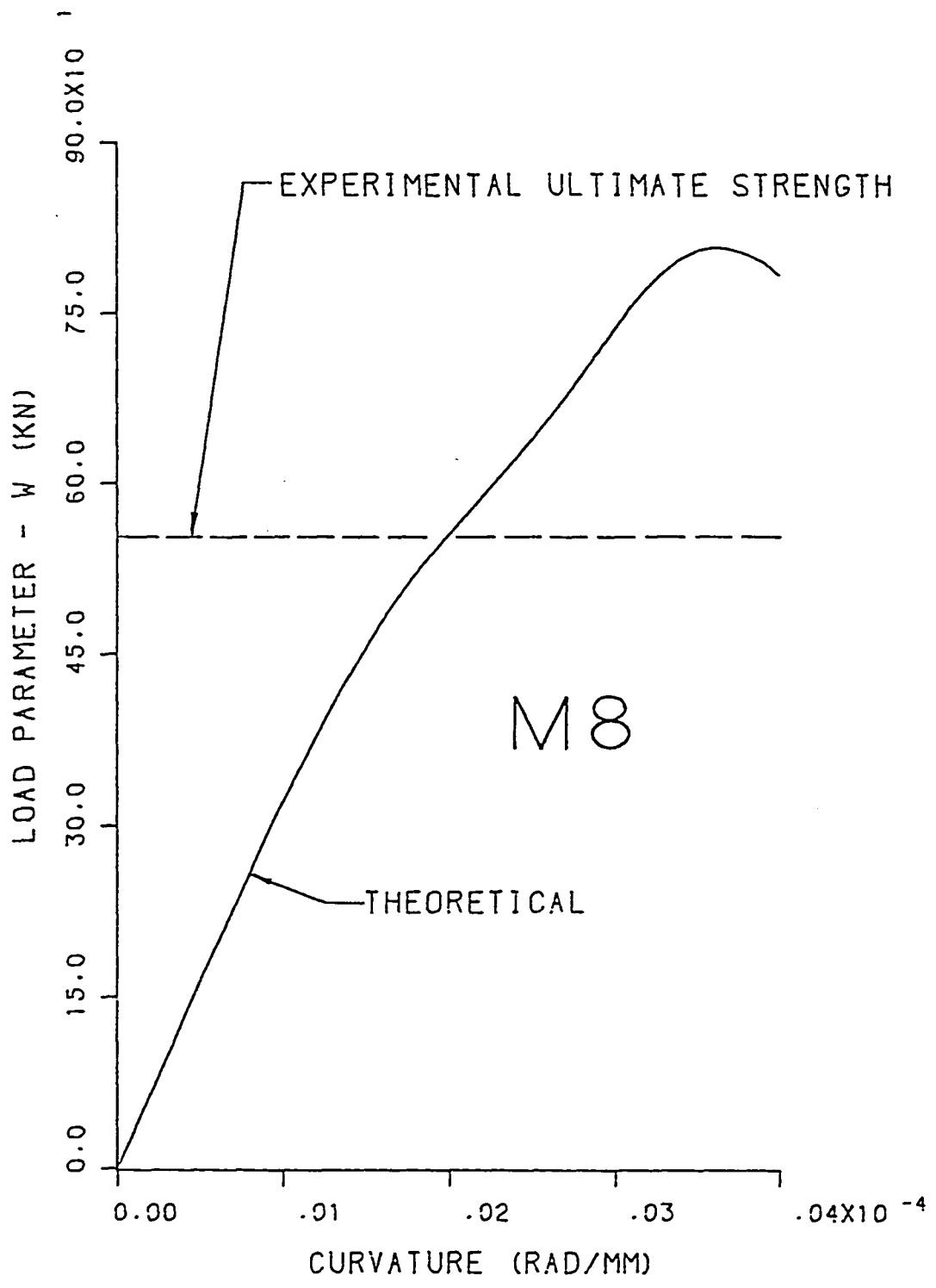Fig.22   Imperial College — Model 8
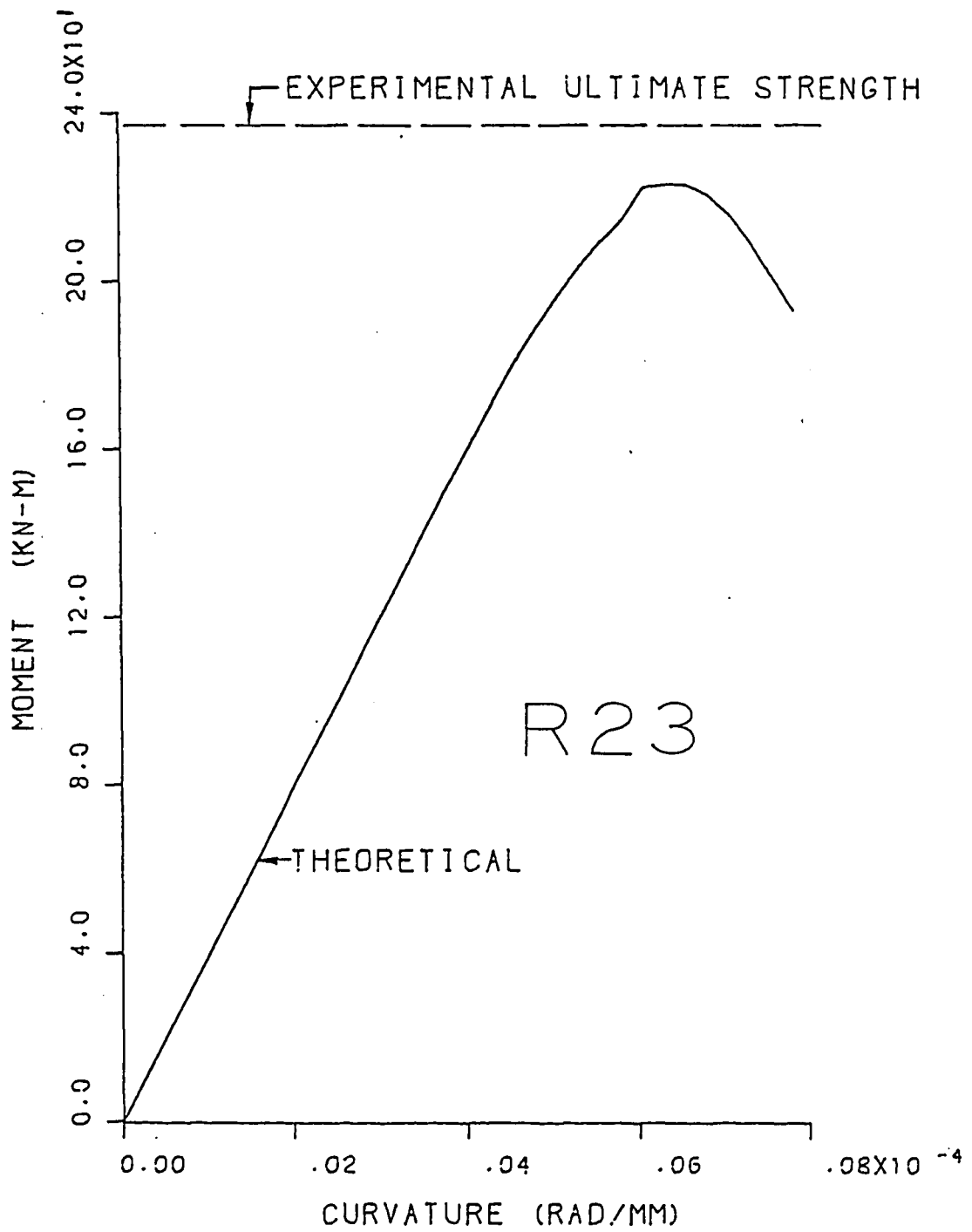
77

Fig.22   Imperial College – Model 8
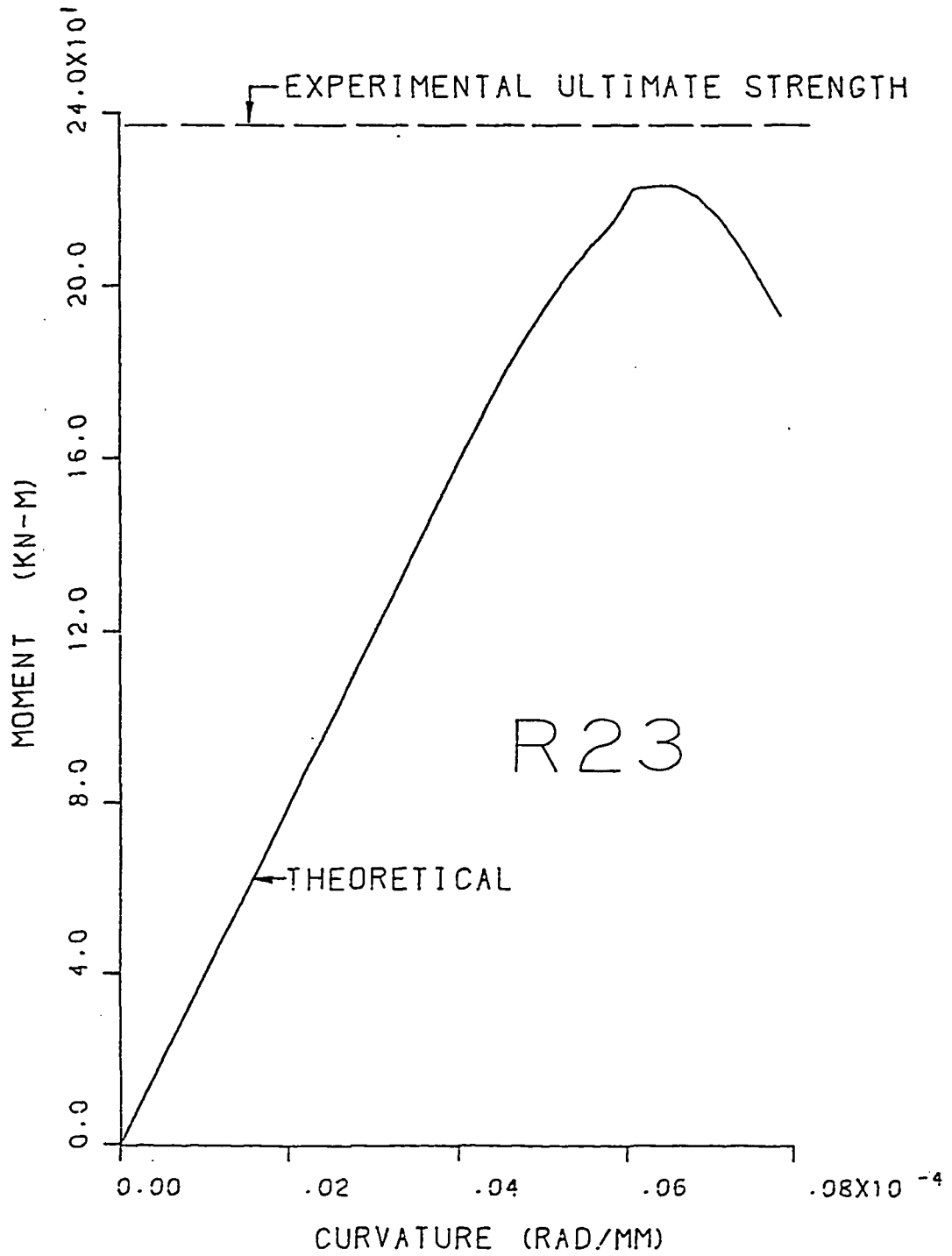
77

Fig.23 Reckling – Test 23

Fig.23   Reckling – Test 23

10. REFERENCES

[1] Becker, H., and Colao, A.
     Compressive Strength of Ship Hull Girders; Part Ill, Theory
         and Additional Experiments.
     Technical Report SSC 267, SNAME Ship Structure Committee,
         1977.

[2] Billingsley, D.W.
     Hull Girder Response to Extreme Bending Moments.
     The Society of Naval Architects and Marine Engineers :51-63,
         June, 1980.
     Discussions by P.Y. Chang (Chang 1980), J.B. O'Brien and W.P.
         Glennie (O'Brien 1980), J.C. Adamchak (Adamchak 1980),
         D.G. Faulkner (Faulkner 1980), and S.G. Stiansen (Stiansen
         1980).

[3] Caldwell, J.B.
     Ultimate Longitudinal Strength.
     In Proceedings, Vol. 107, pages 411-418. Royal Institution
         of Naval Architects, London, 1965.

[4] Dow, R.S., Hugill, R.C., Clark, J.D., Smith, C.S.
     Evaluation of Ultimate Ship Hull Strength.
     In Extreme Loads Response Symposium, pages 133-148. Society
         of Naval Architects and Marine Engineers, New York,
         October, 1981.
     Proceedings of the SSC-SNAME Symposium held in Arlington, VA,
         on October 19-20, 1981.

[5] Dowling, P.J., Chatterjee, S., Frieze, P.A., Moolani, F.M.
     Experimental and Predicted Collapse Behavior of Rectangular
         Steel Box Girders.
     In Penelope Cartledge, BSc (editor), Steel Box Girder
         Bridges, pages 77-94. The Institution of Civil Engineers,
         London, February, 1973.

[6] Dwight, J.B.
     Collapse of Steel Compression Panels.
     In Rockey, K.C., Bannister, J.L., and Evans, H.R. (editor),
         Developments in Bridge Design and Construction, pages
         519-539. Crosby Lockwood, London, 1971.

[7] Herzog, M.
Ultimate Strength of Longitudinally Stiffened Plates
According to Test Results-Consideration of Initial
Imperfections and Residual Stresses (in German: Die
Traglast Einseitig Laengsversteifter Bleche mit
Imperfektionen und Eigenspannungen unter Axialdruck nach
Versuchen).
Verein Deutscher Ingenieure-Zeitung 118(7), 1976.

[8] Herzog, M.
Ultimate Strength of Steel Box Girders (in German: Die
Traglast verstreifter Kastentraeger aus Baustahl).
Bauingenieur 52:57-61, 1977.
Paper presented to the symposium held in April 29, 1976 in
University College, London.

[9] Koiter, W.T.
The Effective Width of Flat Plates for Various Longitudinal
Edge Conditions at Loads Far Beyond Buckling Load (in
Dutch).
Technical Report S-287, National Luchtvaartlaboratorium,
Netherlands, 1943.

[10] Kondo, J.
Ultimate Strength of Longitudinally Stiffened Plate Panels
Subjected to Combined Axial and Lateral Loading.
Fritz Engineering Laboratory Report No. 248.13, Lehigh
University, 1965.

[11] Lee, T.
Elastic-Plastic Analysis of Simply Supported Rectangular
Plates Under Combined Axial and Lateral Loading.
Fritz Engineering Laboratory Report No. 248.7, Lehigh
University, 1961.

[12] Little, G.H.
Stiffened Steel Compression Panels -- Plate Failure Results
for Plain Flat Stiffeners and T-Section Stiffeners.
Technical Report, Birmingham University, Jul, 1977.
Unpublished Preliminary Report.

[13] Maquoi, R.
Theoretical and Experimental Study of the Post-Buckling
    Strength of Stiffened Flanges of Steel Box Girder Bridges
    under Compression (in French:Etude Theorique Et
    Experimentale De La Resistance Post-Critique Des Semelles
    Comprimees Raidies Des Ponts Metalliques En Caisson).
Technical Report 54, Faculte des Sciences, Universite de
    Liege, 1975.

[14] Massonnet, Ch.E., and Maquoi, R.J.
Design of Steel Plate and Box Girder Bridges.
Journal of Struc. Div., ASCE 101(11, Tech. Note, Proc. Paper
    11686):2477-2482, 1975.

[15] Moxham, K.E., and Bradfield, C.D.
The Strength of Welded Steel Plates under Inplane
    Compression.
Technical Report CUED/C-Struct/TR.65, University of
    Cambridge, Department of Engineering, 1977.

[16] Ostapenko, A., and Chern, C.
Ultimate Strength of Longitudinally Stiffened Plate Girders
    under Combined Loads.
In IABSE Proceedings, Vol. 11 Design of Plate and Box Girders
    for Ultimate Strength, pages 301-313. IABSE, London,
    1971.

[17] Ostapenko, A., and Vaucher, A.
Ultimate Strength of Ship Hull Girders under Moment, Shear
    and Torque.
Fritz Engineering Laboratory Report No. 453.6 (MARAD Report
    MA-RD-940-80077), Lehigh University, July, 1980.

[18] Ostapenko, A.
Shear Strength of Longitudinally Stiffened Plate Girders.
In Proceedings, pages 36-40. Structural Stability Research
    Council, Lehigh University, Bethlehem, Pa., 1980.

[19] Ostapenko, A.
Strength of Ship Hull Girders under Moment, Shear and Torque.
In Extreme Loads Response Symposium, page 149-166. Society
    of Naval Architects and Marine Engineers, New York,
    October, 1981.
Proceedings of the SSC-SNAME Symposium held in Arlington, VA,
    on October 19-20, 1981.

81

[20] Ostapenko, A. and Surahman, A.
      Structural Element Models for Hull Strength Analysis.
      Fritz Engineering Laboratory Report No. 480.6, Lehigh
        University, September, 1982.

[21] Ostapenko, A., and Chen, Y.
      Effect of Torsion on Strength of Ship Hulls.
      Fritz Engineering Laboratory Report No. 468.11 (MARAD Report
        No. MA-RD-940-81076), Lehigh University, November, 1982.

[22] Ostapenko, A.
      Steel Box Girders Subjected to Torsion, Bending and Shear.
      In Proceedings of the SSRC Annual Technical Meeting.
        Structural Stability Research Council, Bethlehem, PA,
        1982.

[23] Ostapenko, A., Chen, Y., Vaucher, A., and Moore, T.R.
      Computer Program for Ultimate Strength Analysis of Ship Hulls
        Subjected to Moment, Torque and Shear.
      Fritz Engineering Laboratory Report No. 479.4 (MARAD Report
        No. MA-RD-940-82061), Lehigh University, November, 1982.

[24] Parsanejad, S., and Ostapenko, A.
      Ultimate Strength Analysis of Plate Grillages under Combined
        Loads.
      Fritz Engineering Laboratory Report No. 323.11, Lehigh
        University, 1972.

[25] Rockey, C.K., Evans, H.R., and Porter, D.M.
      A Design Method for Predicting the Collapse Behavior of Plate
        Girders.
      In Institution of Civil Engineers (editor), Proc.
        Institution of Civil Engineers, Part 2, Vol.65, pages
        85-112. Institution of Civil Engineers, London, March,
        1978.

[26] Rutledge, D.R., and Ostapenko, A.
      Ultimate Strength of Longitudinally Stiffened Plate Panels
        (Large and Small b/t, General Material Properties).
      Fritz Engineering Laboratory Report No. 248.24, Lehigh
        University, 1968.

[27] Rutledge, D.R.
Computer Program for Ultimate Strength of Longitudinally
   Stiffened Panels.
Fritz Engineering Laboratory Report No. 248.23, Lehigh
   University, 1968.

[28] Smith, C.S., Kirkwood, W.C., McKeeman, J.L.
Evaluation of Ultimate Longitudinal Strength of A Ship's
   Hull.
AMTE(S) R 671, Admiralty Marine Technology Establishment,
   November, 1977.

[29] Smith, C.S.
Influence of Local Compressive Failure on Ultimate
   Longitudinal Strength of a Ship's Hull.
In International Symposium on Practical Design in
   Shipbuilding, pages . , Tokyo, October, 1977.

[30] Vasta, J.
Lessons Learned from Full Scale Structural Tests.
Transactions of SNAME 66:165, 1958.

[31] Vernarr, J.D.
Comparison Study of Plate Girder Ultimate Strength Methods.
Fritz Engineering Laboratory Report No. 354.454 (Report for
   CE 481), Department of Civil Engineering, Lehigh
   University, September, 1977.

VITA

The author was born in Sunbury, Pennsylvania on August 10, 1956 as the first child of Robert J. and Clara Lee Moore.

He graduated from Cedar Cliff High School in Camp Hill, Pa. in June 1974. In September 1976, he entered Lehigh University and in October, 1980, he received the degree of Bachelor of Science in Civil Engineering.

In September 1981, he enrolled at Lehigh University for the Master of Science program in Civil Engineering where he was Research Assistant on the project Ultimate Strength of Ship Hull Girders (Project 479).